PEP-X Light Source at SLAC
Status Report

Revision 0

June 10, 2008

PEP-X Study Group:

Karl Bane, Lynn Bentson, Kirk Bertsche, Sean Brennan, Yunhai Cai, Alex Chao, Scott DeBarger, Valery Dolgashev, Robert Hettel,, Xiaobiao Huang, Zhirong Huang, David Kharakh, Yuri Nosochkov, Thomas Rabedeau, James Safranek, John Seeman, Joachim Stöhr, Gennady Stupakov, Sami G. Tantawi, Lanfa Wang, Min-Huey Wang, Ulrich Wienands (SLAC, Menlo Park, California), Ingolf Lindau (Stanford University, Stanford, California), Claudio Pellegrini (UCLA, Los Angeles, California)

PEP-X Light Source at SLAC - Status Report

Table of Contents

Executive Summary

SSRL is developing a long-range plan to transfer its evolving scientific programs from the SPEAR3 light source to a much higher performing synchrotron source. The new source would have an order of magnitude higher average brightness and flux in the 1- Å wavelength range than any existing or future storage ring sources planned for the next decade around the world. This enhanced capability will enable new science and faster data acquisition while benefitting from the inherent stability of a storage ring light source. The new source would be housed in the 2.2-km PEP-II tunnel and utilize many but not all of the PEP-II accelerator components and systems. Following the PETRA-III model, PEP-X will have a hybrid lattice where two of its six arcs contain DBA (double-bend achromat) cells that provide a total of ~32 straight sections for insertion device beam lines extending up to 140 m into two new experimental halls (~125,000 sq. ft. each, including lab-office space as shown in Figure ES.1) and the remaining arcs contain TME (theoretical minimum emittance) cells. Beam lines up to 250 m can be accommodated in each hall if the source is situated at the upstream end of the adjacent 120-m long straight section. Beam lines up to 600 m could be located in the PEP arc 1 area.

Using ~90 m of damping wigglers, the horizontal emittance at a 4.5-GeV operating energy with low stored beam current is 0.09 nm-rad. The emittance coupling can be adjusted to produce a
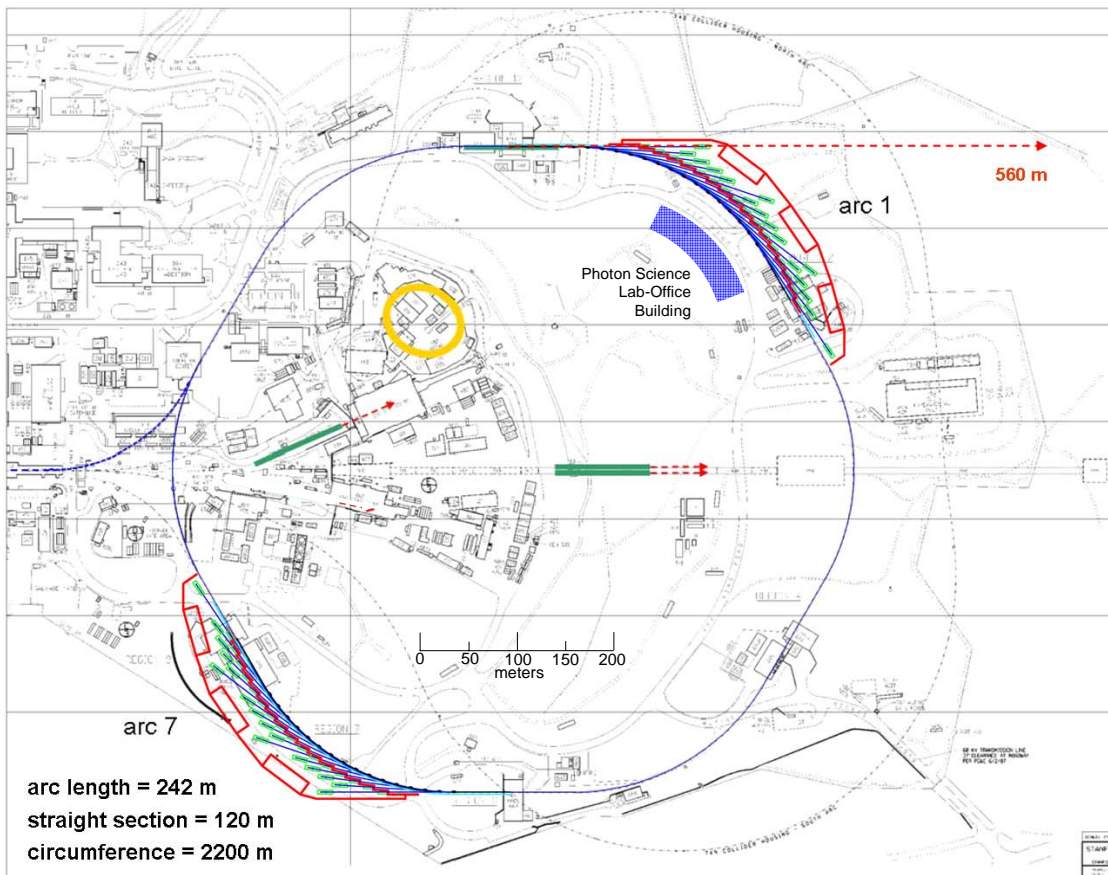
Figure ES.1: Conceptual layout of PEP-X light source with two experimental halls containing ~32 x-ray beam lines, up to 140 m long, with long beam lines (~560 m) accommodated in arc 1. SPEAR3 is shown in yellow; green rectangles represent existing and future FEL undulators for the LCLS. A future lab-office building for Photon Science is also indicated (in block form, not included in the PEP-X proposal).

Brightness Envelopes
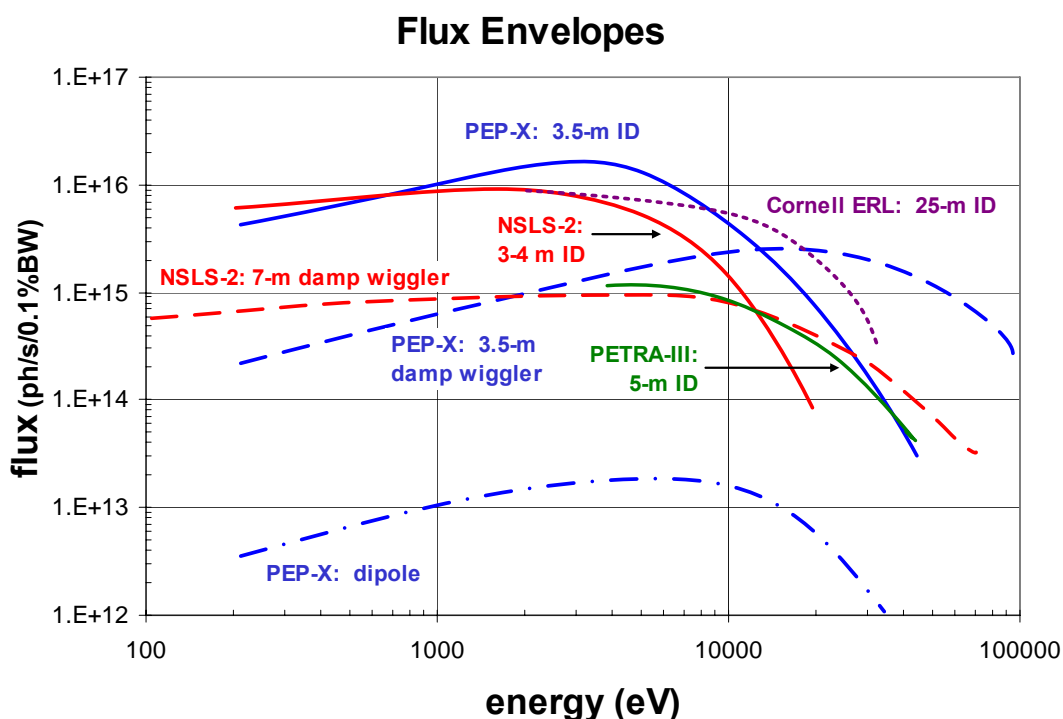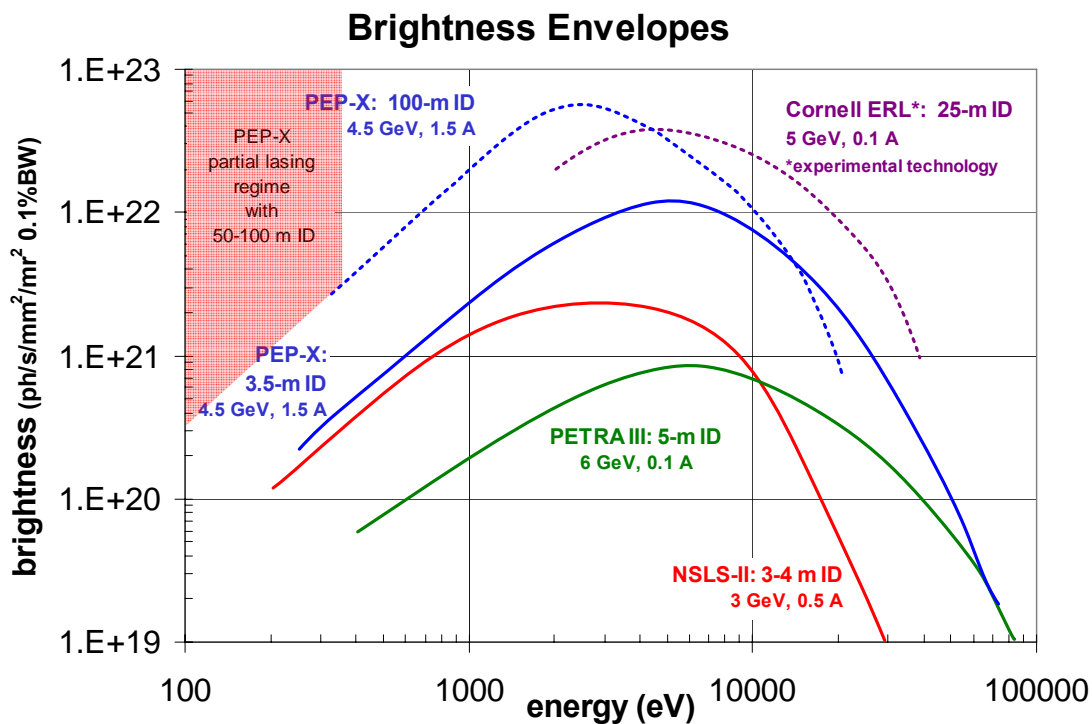
Flux Envelopes

Figure ES.2: Approximate brightness and flux envelopes for PEP-X and other present and future light sources. Partial lasing in a 50 to 100-m ID may be possible at energies <360 eV, increasing brightness by one or two orders of magnitude. The envelope for the futuristic Cornell ERL [6], presently an experimental R&D project, assumes a 25-m ID operating in either high-flux mode (100 mA) or high-coherence mode (25 mA); its spectrum extends to energies higher than shown. PEP-X brightness may be enhanced by a factor of ~2 with optimized lattice parameters at ID straight sections and using high-performance IDs.

vertical emittance of 8 pm-rad, the diffraction-limited emittance for 1-Å radiation. With this coupling, the horizontal emittance grows to 0.14 nm-rad when the beam current is increased to the nominal 1.5-A operating value due to intrabeam scattering within each bunch. The emittance growth due to intrabeam scattering is a function of electron energy, becoming more significant as energy is reduced. The 4.5-GeV operating energy presently chosen in our study represents a first-order optimization of overall spectral brightness in the 1-20 keV range (Fig. ES.2) given intrabeam scattering effects (Sec. 2.6). In future studies, operating energies in the 4-5 GeV range will be more thoroughly investigated to determine if the spectral brightness envelope for this photon energy range can be more optimally balanced.

While the accelerator rf and vacuum chamber systems can operate with an electron current of up to 3 A, the operating current of 1.5 A was chosen for stable multibunch operation, minimal emittance growth due to intrabeam scattering, and to limit the angular power density from undulator sources to 1 MW/mrad^2, a value that can be handled by present-day beam line optical components situated ~50-60 m from the source. Due to the short beam lifetime at these currents (<1 hr) for small vertical coupling, frequent top-off injection, on the order of once per second(s) is necessary to maintain percent-level current constancy. A 3rd harmonic rf cavity will be used to increase the electron bunch length to improve lifetime; lifetime can be further improved by increasing the vertical coupling.

Advances in beam line optical design, including mirrors, refractive optics, monochromators, and other components will be required beyond existing technology to maximally exploit the low-emittance, high-brightness and high-power photon beams generated in PEP-X. Beam stability on the order of a micron or less between source and experiment will be required which is attainable only with advanced electron orbit and beam line stabilizing feedback systems.

Beyond the baseline brightness performance of ~10^{21}-10^{22} (ph/s/mm^2/ mrad^2/0.1% BW) using 3-4 m insertion devices, studies indicate that a 50-100-m undulator, possibly serving as a significant fraction of the damping wiggler and operating with the stored electron beam, could have FEL gain and brightness enhancement of a factor of 10-100 at soft x-ray wavelengths (> ~3.5 nm, < ~360 eV). For the shortest lasing wavelengths, the emittance must be kept below ~0.1 nm-rad and the peak bunch current must be 270 Apk (~1 mA average), values that might be reached by fully coupling the beam (Sec. 3.3), but that might be prevented by bunch instability induced by coherent synchrotron radiation (Sec. 2.7).

As is being explored for present-day storage ring light sources, rf crab cavities or other beam manipulation systems can be used to reduce bunch length in a section of the ring to the order of 1 ps or less (Sec. 4.1.10). In one extreme implementation, rf deflecting cavities might be used to exchange longitudinal and vertical electron beam emittances to produce very short bunches (<100 fs) at the expense of large vertical beam size (several millimeters).

The long-range plan for SLAC is to replace SPEAR3 with PEP-X as a light source by about 2020, with the entire SSRL program migrating to PEP-X around that time. This timescale calls for a start of conceptual design funding by 2014 or earlier.

Nominal source parameters are given in Table ES.1

Table ES.1: Machine parameters for PEP-X 2-DBA/4-TME lattice implementation.

Parameter	Value
Energy	4.5 GeV
Current (operating/max)	1.5 / 3.0 A
# Bunches	3400
Harmonic number	3492
RF frequency	476.00 MHz
Circumference	2199.32 m
Damping wiggler length/period	89.3 m / 10 cm
Horizontal emittance @ 0A/1.5A (ε_y = 8 pm-rad)	0.094 / 0.14 nm-rad
Beta at ID straight center* (x/y)	9.09 / 8.14 m
Beam size @ ID center, I = 1.5 A (x/y)	36 / 8 μm rms
Beam diverg @ ID center, I=1.5 A (x/y)	4 / 1 μrad rms
Bunch length (without/with harm cav)	2.5 / 5.0 mm rms
Lifetime @ 1.5A, ε_y = 70 / 8 pm-rad (5-mm bunch)	57 / 19 min
ID straight section length in arcs	4.3 m
# ID straights in arcs	30
Long straight section length	120 m
# Long straight section for IDs	2

* Betatron amplitudes in ID straights will be optimized for high source brightness and small horizontal beam size in on-going lattice development.

The following report summarizes the present status of the PEP-X design study. The study group has focused primarily on developing the very low storage ring magnet lattice and analyzing the associated dynamical properties of the electron such as lifetime and dynamic aperture. Preliminary analyses of photon beam properties, and the associated requirements for beam line components needed to preserve those properties, have been conducted based on the evolving electron beam parameters. Less time has been invested in the specification of engineering requirements for accelerator and beam line components; nevertheless, first-order estimates of these requirements and very preliminary implementation ideas are presented.

There are many challenging design tasks associated with achieving the design goals for the electron and photon beams for PEP-X. The primary design challenges are associated with creating a viable and workable very low-emittance accelerator lattice, reaching the requisite electron beam stability (in all dimensions, spatial, temporal and spectral) and the ability to deliver the superb properties of each high-power photon source to the user's experimental station with a minimal degradation. R&D activities to accomplish design goals include:

1. Developing a magnet lattice with optimized photon source betatron parameters that has sufficient dynamic aperture for efficient injection and adequate beam lifetime (Sec. 2).
2. Understanding the effects of coherent synchrotron radiation (CSR) on beam dynamics and developing remedies for those effects (Sec. 2.7).
3. Developing high power, high resolution beam line optical components (Sec. 4.2.5).
4. Developing photon absorber designs and geometries for high-power damping wiggler radiation.
5. Developing high performance electron and photon beam position monitor systems.

6. Developing precision electron orbit and photon beam trajectory feedback systems, including highly stable and actively stabilized accelerator and beam line components.

7. Designing an effective 3rd harmonic rf bunch-lengthening cavity system (Sec. 4.1.6).

8. Improving multibunch and rf feedback systems to act effectively when a 3rd harmonic bunch-lengthening cavity is operating.

9. Developing practical rf beam manipulation components for creating short bunches (Sec. 4.1.10).

10. Continuing studies of unseeded and seeded lasing in long soft x-ray undulators.

The combined R&D effort for these topics will involve 10-30 full-time equivalents plus material and service costs over several years. The specification, prioritization, and funding requirements for these activities will be determined in the future.

The scientific case for PEP-X is not included in this report, but will be addressed by a SLAC study group within the next year.

All electron and photon beam parameters and component implementation requirements presented in this report are subject to change and further optimization.

1. Overview

1.1. Long Range Goals for SSRL

SSRL provides 3rd generation storage ring-based synchrotron radiation and experimental x-ray facilities optimized for selected x-ray techniques and scientific areas to a broad scientific user community. The near-to-medium term SSRL program is based on the storage ring SPEAR3, which in 2003 was upgraded to an intermediate energy (3 GeV) high-brightness source. SPEAR3 enhances existing programs and facilitates the development of new scientific capabilities based on micro- or nano-sized x-ray beams with high intensity and high brightness, well defined polarization and time structure in the picosecond range. New instruments and methodologies which utilize these opportunities, coupled with incremental improvements in SPEAR3 performance, like top-off and higher current operation, are the highest near term goals. The *storage ring* concept underlying SPEAR3 which is complementary to LCLS is broadly used at existing x-ray user facilities around the world. Storage rings provide a sure path towards obtaining detailed information on the fundamental interactions between the electrons, spins and atoms in matter "near equilibrium". An improved understanding of these interactions forms a large part of what we envision as "grand scientific challenges" today and SPEAR3 remains a vital tool in our pursuit of many, but not all, aspects of these questions.

The physical size (circumference) of SPEAR3 constitutes a barrier to upgrading it to achieve significantly higher brightness, a direction increasingly driven by the need to study complex materials on the nano-scale. Therefore the longer term future of SSRL is based on the transfer of the evolving scientific programs from SPEAR3 to a higher-performing synchrotron source. To be viable, such an evolution must result in transformational new capabilities measured on an international scale. In order to avoid a "dark period" for the SSRL user community and maintain one of the three vibrant and essential elements of photon science at SLAC (the other two being LCLS and the Centers of Excellence), we envision an adiabatic transition from SPEAR3 to a future state-of-the-art storage ring: PEP-X.

The scientific need for PEP-X is based on its ability to deliver an unprecedented *average* brightness. This allows the study of complex materials, the foundation of advances in key areas of societal impact like energy, environment, health and technology, in an unprecedented phase space, simultaneously covering the fundamental degrees of freedom of space, time and energy. In the past, x-rays have been known for their ability to yield information on atomic and nanoscale length scales through diffraction and imaging. On larger length scales, ranging from microscopic to macroscopic dimensions, spectroscopic techniques have revealed details of the electronic structure through energy and time resolved x-ray measurements. The new scientific paradigm, however, is the recognition of the complexity of matter derived from nanoscale ordering in the charge and spin degrees of freedom and their as yet ill understood dynamics. Such order exists either naturally in macroscopic "correlated materials" or, more generally, in nanoscale materials and liquids through imposed spatial constraints. At present we have only seen the tip of the iceberg because we lack the ability to probe real materials on the nanoscale with energy and time resolved spectroscopies. For example, future studies will focus on the determination of the electronic structure of distinct nanoscale regions by (spin resolved) photoemission spectroscopy or the unveiling of the dynamic behavior of nanoscale regions through x-ray correlation spectroscopy (coherent scattering) that extends well below the

timescale of seconds presently needed for imaging. Such problems are at the very heart of the "grand challenges" identified by BESAC.

The future of x-ray science lies in the use of two complementary sources, x-ray lasers which emphasize *peak* brightnesss (coherence) and the ultrafast *time* domain, and ring based sources which emphasize *average* brightness (coherence) and ultrahigh *energy* resolution. While linac based sources may also produce very high average brightness by combining peak brightness with moderate repetition rates (up to 100 kHz), ring based sources purposely circumvent the effects of peak photon fields by reducing the number of photons per pulse while operating at high pulse repetition rates (~500 MHz). In addition, ring sources employ pulse lengths in the picosecond range compared to linac based sources which emphasize femtosecond pulses. For many experiments picosecond pulses are ideal because the matching picosecond timescale of the electron-phonon coupling allows the electronic system to remain "cool" during and after the pulse. In addition, the laws of physics allow experiments with high energy resolution. The latter arises from the coupled uncertainties in energy (ΔE) and time (Δt) according to $\Delta E \Delta t \sim 4$ fs eV. Hence a 1 femtosecond pulse corresponds to an energy uncertainty of 4 eV while an energy resolution of 1 meV requires a pulse length longer than 4 ps. PEP-X is therefore complementary to LCLS and its scientific program will be pushing toward the exploration of the combined minimum phase space boundary of 1nm, 1meV and 10ps through nanometer-spectroscopy techniques.

PEP-X would occupy the underground tunnel now occupied by the recently decommissioned PEP-II storage rings used to collide beams to study B-meson decays (Sec. 1.2). The extensive developments for high-current, stable operation in PEP-II that were driven by the high energy physics program, coupled with very low emittance storage ring implementation methods being used for new light source and damping ring designs, provide the possibility of delivering average x-ray brightness exceeding that available from the NSLS-II or PETRA-III by an order of magnitude. The 2.2-km circumference, which includes six 120-m straight sections, enables implementing a very low emittance lattice, limited by intrabeam scattering in the electron bunches, to the order of 0.1 nm-rad for 4.5-GeV electron energy. The vertical emittance can be reduced by lattice coupling adjustment to 8 pm-rad, the diffraction limited emittance for 1-Å photons. PEP-X would operate with a nominal beam current of 1.5 A, limited by the power handling capability of beam line optical components, making use of the powerful PEP-II rf system capable of sustaining beam currents in excess of 3 A at this energy. Studies indicate that with such a low emittance, FEL gain and brightness enhancement at soft x-ray wavelengths would be attained with the stored beam. Such a source would complement the LCLS science program and offer exciting and groundbreaking scientific opportunities, including:

- imaging with 1-nm or smaller spatial resolution with sufficient intensity
- combination of nm spatial and meV energy resolution: "nano-ARPES"
- combination of nm spatial with temporal resolution down to micro or nanoseconds: soft x-ray photon correlation spectroscopy
- spin polarized photoemission (now limited by 10^{-4} detection efficiency) with adequate intensity
- x-ray Raman spectroscopy or "x-ray-loss XAFS" of low-Z systems in small volumes and under extreme conditions

We envision PEP-X to replace SPEAR3 by about 2020, with the entire SSRL program migrating to PEP-X around that time. This timescale calls for a start of conceptual design funding by 2014 or earlier.

1.2. PEP-II Facility

The PEP-II accelerator facility consists of two storage rings: the 9-GeV, 2-A High Energy Ring (HER) and the 3.1-GeV, 3-A Low Energy Ring (LER) housed in a 2.2-km circumference tunnel having six 243-m arcs and six 120-m straight sections (Fig. 1.2.1). The LER is mounted ~0.9 m directly above the HER. Both lattices consist of 16 FODO cells per arc. There are only short (~0.5 m) empty straight sections in the HER arcs due to the long dipole magnets. The BaBar particle physics detector is located in Interaction Region 2 (IR-2) where special ring lattice and vacuum chamber features enable the beams

Figure 1.2.1: PEP-II with functions of the straight sections indicated in black for the 9-GeV electron HER and in red for the 3-GeV positron LER.

from the two rings to collide. PEP-II operated as a B-factory for the US DOE High Energy Physics program from May 1999 until April 7, 2008.

The PEP-II facility is equipped with mode-damped RF cavities (28 for the HER, 8 for the LER) powered by 15 klystron power stations, transverse and longitudinal multibunch feedback systems, injection components, vacuum system components, magnet power supplies, and a facilities infrastructure for cooling water, compressed gas and mains power. While PEP-II has a complete complement of instrumentation and control systems, it is likely that most of them will become obsolete or difficult to maintain in a future light source implementation and will need to be replaced.

Electrons for the HER and positrons for the LER are provided by the main SLAC linac and are transported to the rings via two transfer lines: the North Injection Transport (NIT) line for electrons circulating clockwise in the HER, and the South Injection Transport (SIT) line for positrons circulating counterclockwise in the LER. "Trickle charge" single-bunch injection at about 10 Hz (30 Hz possible) is provided for both rings to maintain a high degree of stored current constancy.

The nominal emittance for the HER is 48 nm-rad at 9 GeV respectively. By increasing the phase advance per HER lattice cell from 60° to 90° and reducing the ring energy to 4.5 GeV, the HER ring emittance can be reduced to 5 nm-rad; adding ~100 m of damping wiggler further reduces the emittance to 0.8 nm-rad. Increasing the phase advance per cell reduces the emittance even further, but the strong sextupoles that would be required reduce the dynamic aperture to an unacceptably small value. The drawback to this simple implementation is that there are no straight sections for insertion devices in the arcs. For this reason, new lattice configurations are being considered for PEP-X as discussed below.
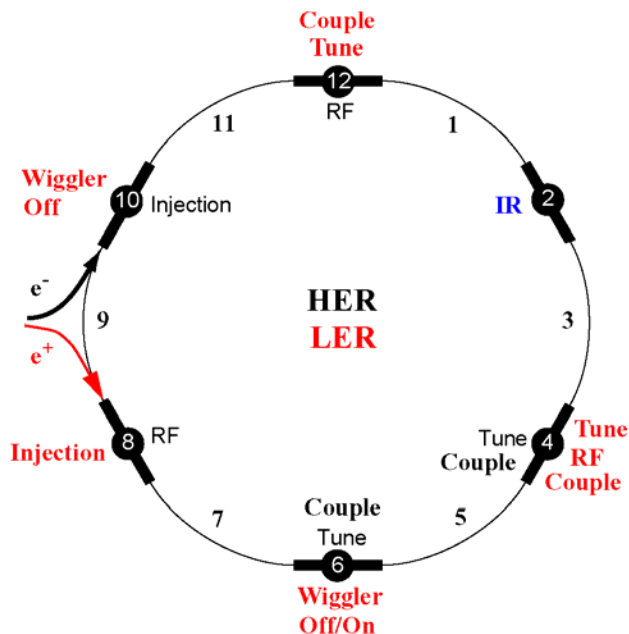
The nominal emittance for the LER is 24 nm-rad at 3 GeV. Due to the short length of the LER dipole magnets, no appreciable reduction in emittance at energies between 3 GeV and the maximum of ~4 GeV is possible except that gained using damping wigglers. For this reason, use of the LER as a light source is not being considered.

1.3. PEP-X Implementation

The predominant goal for PEP-X is to serve as the next high-performance light source at SLAC for the diverse SSRL user community. The parameters and properties that define the performance capabilities of such a light source for providing scientific capabilities discussed in Section 1.1 include:

- high average brightness and flux
- moderate peak brightness and flux
- high coherent flux and photons per pulse
- spectral range and tunability
- photon energy resolution
- spatial measurement resolution
- photon beam size and bunch length
- photon polarization control
- beam line and optical component performance
- beam stability
- different operating modes as needed to accommodate various applications

1.3.1 Light Source Possibilities

The large circumference and six long straight sections provided by the PEP tunnel offer many interesting and potentially novel possibilities for implementing a light source that would achieve very high performance for some or all of the parameters listed above.

The predominant parameter characterizing source performance, brightness B, scales proportionally with photon flux $F(\Delta\lambda/\lambda)$ in a wavelength bandwidth $\Delta\lambda/\lambda$ and inversely with transverse beam emittance for that photon wavelength:

$$B(\Delta\lambda/\lambda) = \frac{F(\Delta\lambda/\lambda)}{4\pi^2 (\varepsilon_x \oplus \varepsilon_r)(\varepsilon_y \oplus \varepsilon_r)}$$

where ε_x and ε_y are the horizontal and vertical electron beam emittances, ε_r is photon emittance from a point source, and $\oplus$ represents the quadrature sum. The two ways to reach high brightness are therefore to 1) reduce the transverse emittance of the electron beam towards the diffraction limit of the point-source photon beam at the wavelength of interest (given by $\lambda/4\pi$, or 8 pm-rad for 1-Å photons), and 2) increase the flux. Flux, and the radiated power that must be handled by beam line optics, increase with beam current and energy. Note that a very low-emittance source can have high brightness but low flux (such as an ERL), and a relatively high emittance source can be bright if the flux is large. In the early stages of the PEP-X design study, several implementation possibilities having different balances of flux and emittance were investigated, including:

- A very low-emittance, high-current storage ring with damping wigglers in place of the HER having an emittance between 1 and 0.1 nm-rad, depending on how much of the PEP-

II HER is replaced, at an energy between 3 and 5 GeV. Vertical emittance would be ~8 pm-rad, at the diffraction limit for 1-Å, 12-keV photons, reached by reducing the horizontal-vertical emittance coupling. This implementation option was ultimately chosen for the base machine proposal (Sec. 1.3.2).

- An ultra-low emittance storage ring (emittance <0.05 nm-rad) in place of the HER, most likely requiring on-axis injection due to a very small dynamic aperture. On-axis injection would necessitate complete bunch or multi-bunch replacement during each injection cycle from either a high-performance linac injector or from an accumulator ring, possibly configured from the LER. Current and flux would be limited by lifetime issues.

- An ultra-low emittance, low-current energy recovery linac (ERL, ~0.01 nm-rad, the diffraction limit for 10-keV photons), possibly co-located in the ring tunnel.

- Soft x-ray FEL lasing capabilities providing high flux on rings having <0.1 nm-rad emittance using a very long (~100 m) undulator (Sec.3.3) Unsaturated SASE from the stored electron beam would enhance the radiated power at the resonant wavelength by a factor of ~100, resulting in an average brightness of ~10^{24}. Saturated lasing at these wavelengths, perhaps in shorter undulators, might be reached with a laser seed source, although sufficiently powerful sources do not yet exist for wavelengths <~10 nm.

Many of these implementation options have been considered by earlier investigators: conversion of PEP-I into a light source was first considered in the mid-1980s to early 1990s [1, 2, 3, 4], a 2-km "ultimate light source" (~0.13 nm-rad @ 7 GeV with 280 m of damping wigglers) was investigated in 2000 [5], multi-GeV ERL light sources are under experimental development at Cornell [6] and elsewhere, and FEL lasing of a 60-m long undulator at 4 nm wavelength in a switched bypass on the converted PEP-I light source was investigated in 1992 [7].

For all ring implementation options, space is available to implement rf electron bunch manipulation components, whether for fast kicking or for bunch phase space manipulation [8, 9]. For example, pulsed and CW rf crab cavities are already being considered for use as localized bunch-length compressors, and 3rd-harmonic rf cavities are used to lengthen bunches in many storage rings in order to increase beam lifetime and to avoid disruptive high-frequency beam instabilities. PEP-X could employ these devices, and potentially other technologies yet to be developed, to enhance light source performance.

1.3.2 PEP-X Base Implementation

Of the implementation options mentioned above, the one that is best matched to meeting future SSRL needs at reasonable cost and risk, in an era where the LCLS provides high peak brightness and short-bunch FEL capability at SLAC, is the first: a very low emittance storage ring having high current and flux and >~24 insertion device (ID) straight sections for x-ray beam lines. While a very low-emittance ERL promises to provide very high
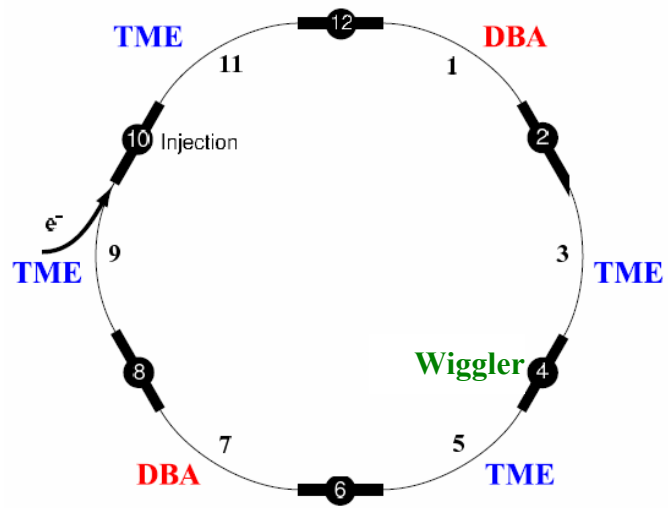
Figure 1.3.1: PEP-X with 2 DBA arcs and 4 TME arcs. Damping wiggler location might change and/or be distributed in two long straight sections.

brightness with less current and total photon power, the technology is highly experimental at this stage and the cost for the high-energy superconducting linac could be prohibitive.

To reach the highest performance and a brightness that is ten times higher than state-of-the art facilities now in construction, the base design for PEP-X replaces almost all of the PEP-II HER lattice and vacuum chamber components. On the other hand, many valuable components from PEP-II including the tunnel, high-performance rf systems, multi-bunch feedback components and facility infrastructure would be reused where possible.

The present magnet lattice for PEP-X consists of two arcs having 16 double-bend achromat (DBA) cells per arc and four arcs having 32 theoretical minimum emittance (TME) cells and 2 matching cells per arc to minimize ring emittance (Fig. 1.3.1). While the arcs with TME cells would have no straight sections for IDs, each of the two DBA arcs would provide 15 straight sections, 4.3 m in length, and an experimental hall for each arc would contain ~16 beam lines nominally 110-140 m long, including one having an ID source located in the upstream long straight section (Fig. ES.1). The beam line for this ID could be up to 250 m long while still contained in the experimental hall by placing the source ID far upstream in the 120-m straight section. There is room in the arc 1 area for longer beam lines, up to ~600 m, that extend beyond the experimental hall (Fig. ES.1). Very long undulators or multiple undulators (in special chicane or gentle arc lattice sections) for beam lines could be located in IR-12 and IR-6 and would provide significant emittance damping.

The 4.5-GeV operating energy for PEP-X has been chosen at this point in the design study as a first-order optimization of the trade-off between brightness at photon energies <~10 keV and the dynamical properties of the electron beam. In principle, the photon brightness below 10 keV would be enhanced as the ring energy E is reduced towards 4 GeV and below provided the beam current I can be increased from that at 4.5 GeV to maintain a constant photon power density on accelerator and beam line components ($I \propto E^{-4}$ for constant power density). In reality, the intrabeam scattering (IBS) increases beam emittance for a given beam current as electron energy is reduced (Sec. 2.6), and this effect negates the potential brightness gain. For PEP-X, the brightness below 10 keV is less at 4 GeV and below than at 4.5 GeV. Lower ring energy also reduces the thresholds for electron bunch instabilities. A more detailed optimization of operating energy will be made in the future, with beam power issues limiting the upper energy reach.

While the accelerator rf and vacuum chamber systems can operate with a current of 3 A at 4.5 GeV, the operating beam current of 1.5 A was chosen for stable multibunch operation and to limit the angular power density from undulator sources to 1 MW/mrad^2, a value that can be handled by present-day beam line optical components situated midway along a 140-m beam line. This power handling capability could conceivably increase in the future as new high-power optics technology is developed, enabling higher current operation in PEP-X (at the expense of increasing emittance from intrabeam scattering within each electron bunch). Due to the short beam lifetime at these currents and small coupling, frequent top-off injection, on the order of every second(s), is necessary to maintain percent-level current constancy. The natural electron bunch length of 2.5 mm rms would be lengthened to 5 mm rms using a 3rd harmonic rf cavity to improve lifetime. Lifetime can be increased further by increasing the vertical coupling.

Machine parameters are summarized in Tables ES.1 and 2.1.1. Nominal photon spectral brightness and flux are shown in Fig. ES.2 for typical 3.5-m IDs in the arcs. Photon source properties are discussed more completely in Section 3. While the horizontal and vertical

betatron amplitudes for the ID straight sections do not provide optimal source properties at the time of this report, it is expected that they will be optimized as lattice studies continue.

The chosen PEP-X implementation is described in more detail in the following sections. These sections summarize the present status of the PEP-X design study; all performance parameters and engineering concepts presented in the report are preliminary and subject to change and further optimization.

2. Accelerator Physics

Based on the discussion in Chapter 1, our primary design goals are:

- Achieving a very low emittance beam of about 0.1 nm-rad at an energy of 4.5 GeV (not including the effect of intra-beam scattering)
- Providing adequate dynamic aperture to accept the electron beam from the existing PEP-II injector
- Storing high beam current up to 1.5 A with adequate lifetime and stability
- Providing at least 24 short-straight and dispersion-free regions in which to place the undulator insertion devices (ID) and maintaining flexibility to change its nearby optics
- Reusing the existing PEP-II tunnel, injector, and rf system

To achieve these challenging goals, we have introduced the following features into our design:

- Theoretical minimum emittance (TME) cells to achieve the very low emittance
- Double bend achromat (DBA) cells to provide spaces for IDs and to retain emittance
- 90-meter damping wigglers to further reduce emittance and damping time
- A powerful low emittance injector to continuously inject electrons into the small acceptance of the ring
- A large number of bunches (~3400) to mitigate the effects of intra-beam scattering, Touschek lifetime, and other single-bunch instabilities
- A large number of rf buckets enables us to have flexible bunch patterns to mitigate the effects due to fast-ion instability (FII)

A more detailed discussion of accelerator physics issues is contained in reference [10].

2.1 Lattice Design

In the PEP-X design, the HER FODO arcs are replaced with two DBA arcs and four TME arcs as shown in Fig. 1.3.1. In addition, a damping wiggler is added to a long straight section to help decrease the emittance. Each DBA arc consists of 16 cells with the optics shown in Fig. 2.1.1. The two DBA arcs provide 30 straight sections for 3 m IDs, where $\beta_x = 9.1$ m, $\beta_y = 8.1$ m. Each
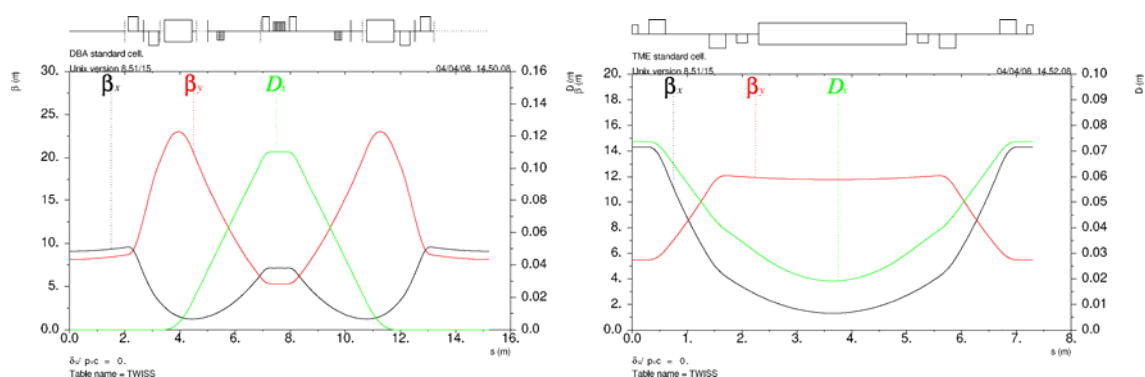
Figure 2.1.1: Optics functions in one DBA cell (left) and one TME cell (right).

TME arc contains 32 regular cells shown in Fig. 2.1.1 and 2 matching cells. In this design, the natural emittance for 6 arcs of TME cells is 0.1 nm at 4.5 GeV, but the combination of 4 TME and 2 DBA arcs results in a higher emittance of 0.37 nm. To reduce the emittance to the 0.1 nm level, the 89.3 m damping wiggler is included in a straight section 4. Depending on practical considerations, it can be also located in straights 2 and 6 without affecting the lattice parameters. The wiggler damping effect is maximized using 10 cm wiggler period and 1.5-T field.

The PEP-X straight sections will contain the injection system, the RF accelerating cavities, the damping wiggler and the tune adjustment system. In this design, 5 straight sections have identical FODO lattice, matched to the DBA or TME arcs and to the damping wiggler. Design of the injection section adopts a vertical injection into the PEP-X because of the larger vertical beam acceptance. The injection section uses the existing HER system, but adds 4 quadrupoles for improved optics match. The injected beam acceptance is maximized by using a high β_y function at the injection point and by moving the stored beam close to the injection septum with bump magnets and fast kickers.

The PEP-X optics functions are shown in Fig. 2.1.2 and the lattice parameters are listed in Table 2.1.1.
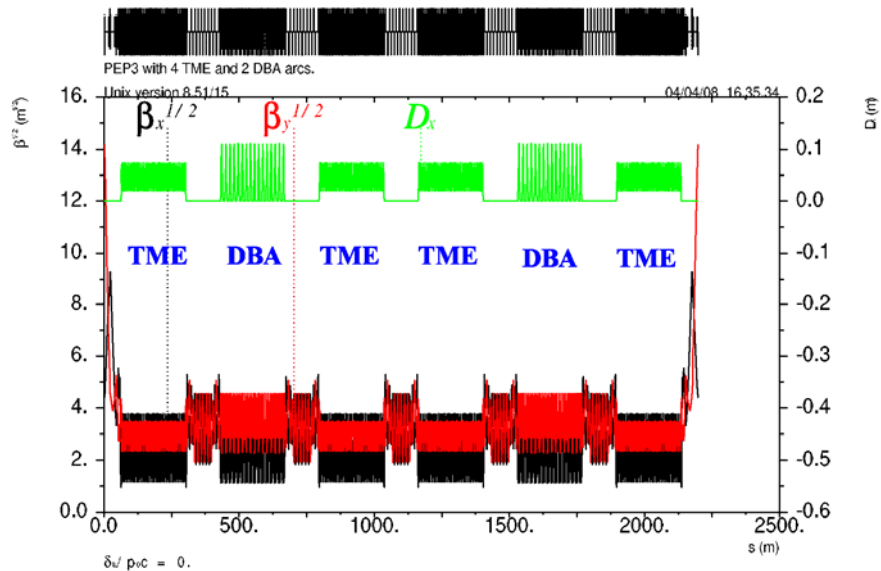
Figure 2.1.2: Optics functions in the complete PEP-X ring.

Table 2.1.1: PEP-X lattice parameters.

Energy, GeV	4.5
Circumference [m]	2199.32
Betatron tune, x/y	86.23 / 36.14
Synchrotron tune	0.00742
Momentum compaction	$4.72 \cdot 10^{-5}$
Emittance without IBS [nm]	0.094
RMS bunch length [mm]	2.50
RMS momentum spread	$1.12 \cdot 10^{-3}$
Damping time, $x/y/s$ [ms]	19.7 / 20.2 / 10.2
Natural chromaticity, x/y	-132.7 / -72.8
Energy loss [MeV/turn]	3.27
RF voltage [MV]	10
Total damp wiggler length [m]	89.325
Damp wiggler period [m]	0.1
Damp wiggler field [T]	1.5
Regular ID straight length [m]	4.26
Number of regular ID straights	30
$\beta x/\beta y$ at ID center [m]	9.09 / 8.14

2.2 Damping Wigglers

The ability of the damping wiggler to reduce emittance is determined by the period length of the wiggler, the peak magnetic field strength, and the total wiggler length. The emittance variation of the damping wiggler as a function of field strength for different wiggler period lengths based on the PEP-X lattice is shown in Fig. 2.2.1. The effects of emittance reduction versus total wiggler length for different wiggler periods are shown in Fig. 2.2.2.
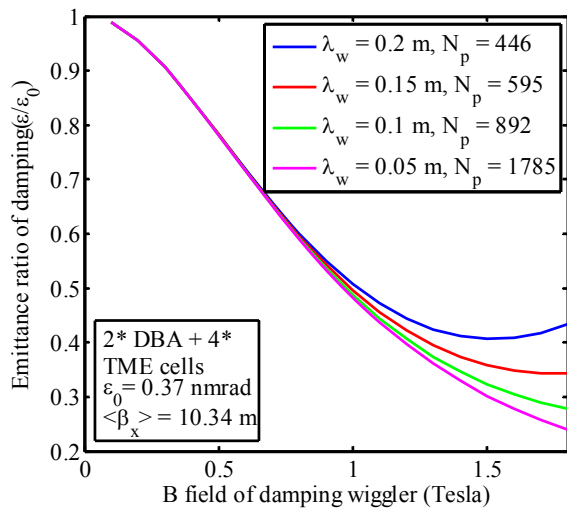
Figure 2.2.1: Emittance reduction of damping wiggler (~90 m) as function of wiggler field strength with different wiggler period length.
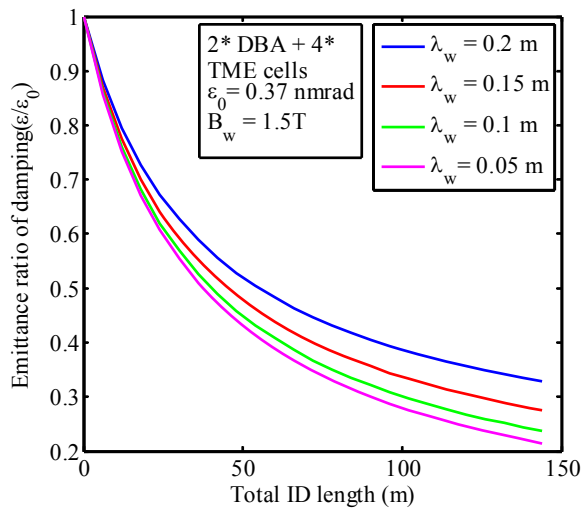
Figure 2.2.2: Effects of emittance reduction versus total wiggler length of different wiggler periods.

The beam emittance for PEP-X without damping wigglers is 0.37nm-rad. Because of the small initial emittance, the optimal parameters of the damping wiggler tend towards short periods and high fields as shown in Fig. 2.2.1. With a period of 10 cm, a peak field of 1.5 Tesla and a total length of 89.3 m, the PEP-X damping wigglers reduce emittance from 0.37 to 0.1 nm-rad. This total damping wiggler length would be comprised of 18 wiggler sections, each 4.96-m long, installed in a long straight section having the FODO optics with a 10.3-m average horizontal beta shown in Figure 2.2.3. The total radiated power from the wiggler is 4 MW with a 1.5-A beam, which must be intercepted with a suitable photon absorber geometry (Sec. 4.1.3).
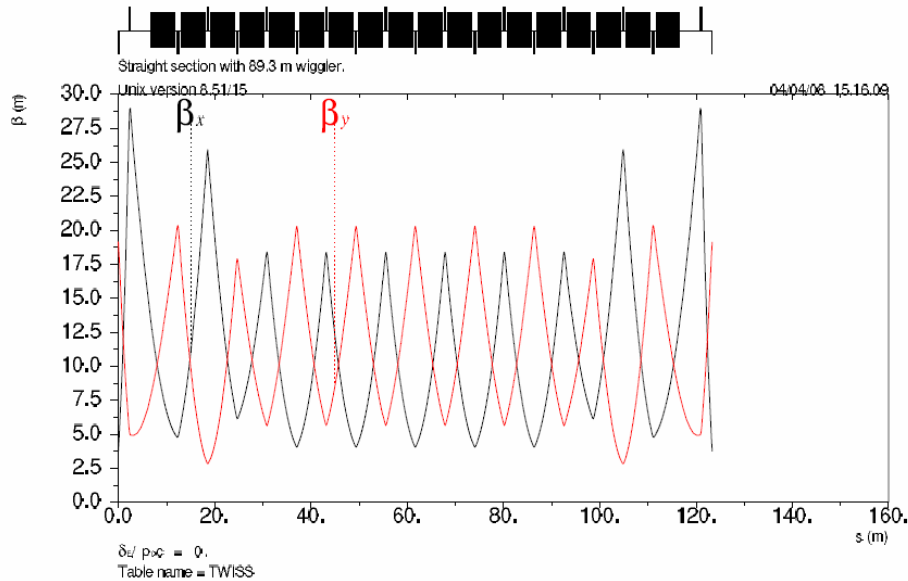
Figure 2.2.3: FODO optics for straight section containing 18 damping wiggler sections, each ~5-m long.

Table 2.2.1 summarizes parameters for different damping wiggler options, including a superconducting implementation that would take advantage of future technology and the possibility of providing a significant fraction of the damping function using a long soft x-ray FEL undulator (Sec. 3.3), reducing the total length of dedicated damping wigglers.

Table 2.2.1: Parameters of damping wiggler for PEP-X, $\langle\beta_x\rangle$ = 10.34 m, J_x =1, ε_0= 0.37 n mrad, total wiggler length is 89.3 m.

period (cm)	peak field (T)	full gap (mm)	wavelength* (Å)	wiggler parameter K	emittance ratio $\varepsilon/\varepsilon_0$
10	1.5	15.4	14.1	-	0.32
Option of partial lasing using damping wiggler					
5	1.27	5.93	60	5.93	0.36
5	0.5	2.33	12	2.33	0.78
Superconducting undulator					
1.4	1.5	1.96	2.6	1.96	0.30

*first harmonic

2.3 Dynamic Aperture

Sextupoles are located where the dispersion is large and the beta functions are well separated so that their strength and effect on dynamic aperture are minimized. The phase advance of the unit cell is also chosen to cancel out the first order terms. The horizontal and vertical phase advances per TME cell are 0.375 and 0.125 in units of 2π, respectively. The phase advances per DBA cell are 0.736 horizontally and 0.238 vertically. A dynamic aperture search by scan of the global tune, set by adjusting the strength of FODO quadrupoles in the long straight section, is shown in Fig. 2.3.1. The working tune of 86.23 and 36.14 are chosen. There are two families of sextupoles. One family, SD and SF, is in the TME cell, and the other, SD1 and SF1, is in the DBA cell. The linear chromaticity is set to zero. The dynamic aperture tracking results with systematic and random magnet errors are also shown in Fig. 2.3.2. The tracking point is set at the injection point. The 3-σ injected beam with injected beam emittance and beta function of storage ring is also shown in the figure. The vertical dynamic aperture is sufficient for the vertical injection.
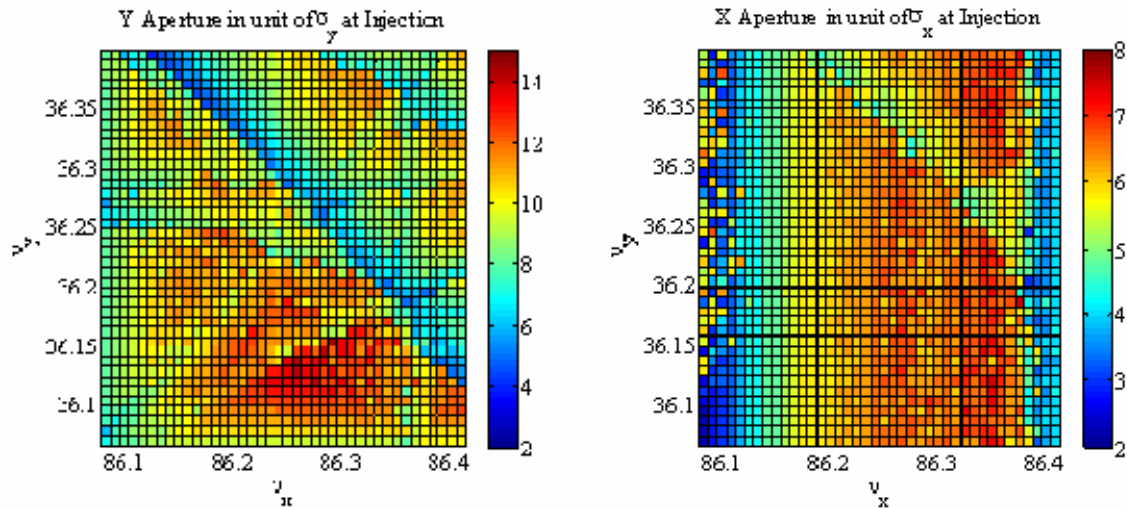
Figure 2.3.1: Scan of dynamic aperture at different working tunes.
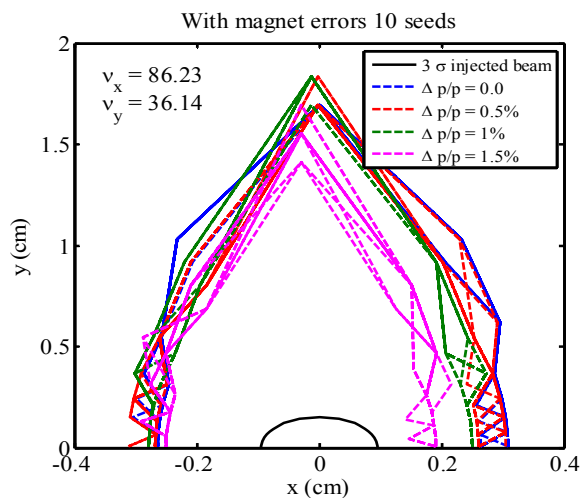
Figure 2.3.2: Dynamic aperture tracking with systematic and random magnetic errors based on the measurements of the PEP-II magnets.

2.4 Injection

At present it is planned to adapt the PEP-II vertical injection scheme for PEP-X. The stored beam will be bumped by four DC bump magnets then kicked by two identical pulsed kickers separated by 180° in vertical betatron phase. The injection aperture should be able to include at least a 6-sigma full width injected beam plus the effective septum width of 4 mm and a 4-sigma half-width stored beam. The beam parameters at the injection point are shown in Table 2.4.1. Injected beam parameters are based on those provided by the present linac and damping ring injector for PEP-II. The phase space diagram at injection point is shown in Fig. 2.4.1. The kick amplitude is 16.1 mm and the injected beam betatron amplitude is 6.23 mm as shown in the figure. The vertical aperture is adequate for these injection parameters. Future study will be determine if vertical injection can be accommodated by the small-gap insertion devices and chambers that create beam loss apertures. If this is a problem, a horizontal injection implementation will be pursued.

Table 2.4.1: Beam parameters at injection.

Vertical injection						
Beam parameters	Energy(GeV)	β_y (m)	α_y	D_y (m)	ε_y(nm rad)	σ_y(mm)
Injected beam	4.5	40	0	0	1.3	0.23
stored beam	4.5	200	0	0	0.185	0.19
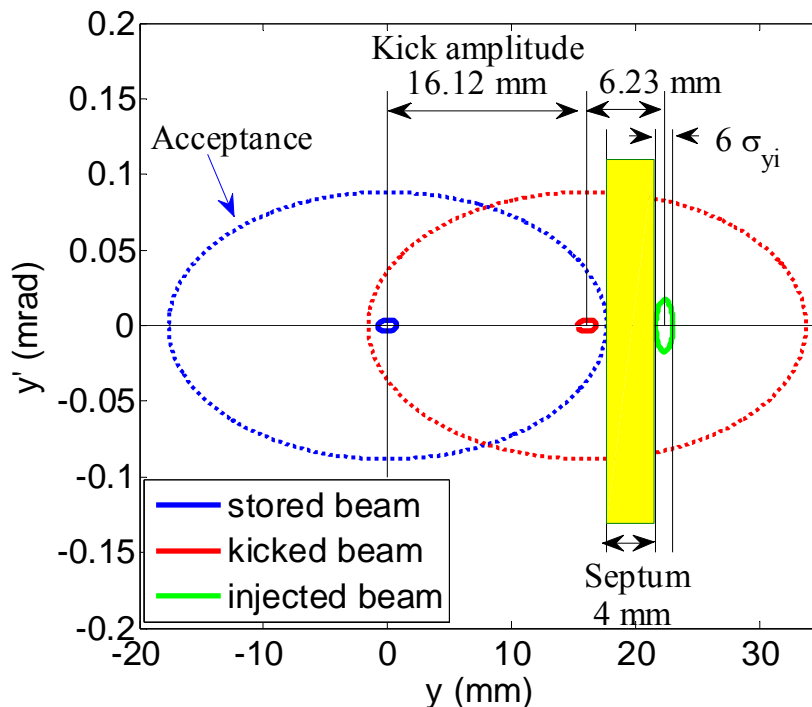
Figure 2.4.1: Phase space diagram of injection acceptance. In this scheme the kick amplitude is the maximum and the injected beam betatron amplitude 6.23 mm is the smallest. The stored beam center is on the closed orbit of a DC bump.

2.5 Stability Requirements

The demanding beam stability requirements for synchrotron light sources include maintaining sufficiently constant photon beam position, angle, size, energy, and, in some cases, photon pulse time-of-arrival, for users to achieve the spatial, temporal and spectral resolution needed for their experiments. Typical specifications for beam pointing stability are 10% of photon beam transverse dimensions, while the longitudinal phase stability requirement may be a small fraction of 1° in order to meet the energy resolution needs ($<5 \times 10^{-5}$) or time-of-arrival jitter needs ($<1ps$) for demanding experiments. Stability requirements are a function of bandwidth, dependent on experiment data integration times, and component specifications must reflect this.

Transverse stability requirements may be modified depending on 1) whether the beam is focused or not; 2) the size of limiting apertures upstream of the experiment (including small slits and collimators); 3) the presence and nature of diffracting and other optical components; 4) whether acquired data are normalized to the instantaneous incident beam intensity. For example, energy-dependent sample absorption measurements may require $<0.1\%$ noise in the data to resolve fine structure in the spectral scans. Without proper intensity normalization, meeting this noise criterion would require a more demanding pointing stability requirements of $<5\%$ of the beam dimensions, and a transverse beam size stability of $<0.1\%$, averaged over the data point acquisition period. In another example, imperfections in a vertically focusing mirror may make it impossible to produce the few-micron vertical spot size of a perfect 1-to-1 imaging system, relaxing the need to stabilize beam position at the source to a small fraction of a micron.

Given the very small photon beam size and divergence of a typical undulator source in PEP-X, extraordinary measures will need to be taken in both the accelerator and beam lines to achieve beam pointing and intensity stability, especially in the vertical plane. These measures include:

- stable design of experimental floor and building
- stable support of magnets and vacuum chambers with nm-level vibration amplitudes and sub-micron-level diurnal stability
- temperature stability on the order of 0.1^oC for critical accelerator and beam line components
- highly stable (order 10 ppm or less) and very low ripple main magnet power supplies
- very high performance beam position monitor (BPM) and orbit feedback systems (beyond the present state of the art) using ultra-stable electron BPMs flanking each insertion device photon source and x-ray BPMs in the beam line
- optical component feedback systems and photon beam intensity monitors in the beam lines to maintain pointing stability and to normalize acquired data to incident intensity
- real-time tune and coupling compensation for scanning insertion devices

Achieving these stringent requirements will require an integrated effort from the accelerator and beam line designers to maintain stability integrity in all aspects of hardware and control system design. It may be necessary to implement high-resolution (~100 nm) mechanical motion/position survey sensors for critical components in the accelerator (e.g. ID BPMs) and beam line (e.g. optical components, small apertures and collimators, etc).

Besides mechanical and electrical stability of the magnets, BPM and beam line components, there are a number of high frequency effects which can drive transverse and longitudinal bunch

motion. These include rf phase and amplitude noise, rf cavity and vacuum chamber impedances, and coherent synchrotron radiation impedances. Mitigations for these effects include high performance low-level rf controls, longitudinal and transverse multibunch feedback systems and low impedance vacuum chamber designs. While it is expected that a third harmonic bunch lengthening cavity will provide Landau damping for coupled oscillations, the bunch lengthened mode may complicate fast rf feedback performance, requiring further rf controls development.

Because of the short beam lifetime, frequent top-off injection will be required for PEP-X (Sec. 2.6). The stored beam orbit transient associated with each injection pulse could degrade beam quality for a user if the orbit transient amplitude (averaged over the user data acquisition integration period) is not reduced to 10% of the very small electron beam dimensions, or unless user data acquisition can be successfully gated with each injection pulse. The interval between injection pulses can be increased by increasing lifetime, reducing current constancy (e.g. 10%, at the expense of requiring multiple 120-Hz injection shots to refill), or by increasing the injected charge per shot. This issue is discussed further in Section 4.1.7.

2.6 Intrabeam Scattering and Touschek Lifetime

Intrabeam scattering (IBS) describes multiple Coulomb scattering that leads to an increase in all beam dimensions and in energy spread, whereas the Touschek effect concerns large single Coulomb scattering events that lead to immediate particle loss. In low emittance machines, such as PEP-X, both effects are important.

We assume PEP-X is coupling-dominated and the vertical emittance is proportional to the horizontal emittance, $\varepsilon_y = \kappa\varepsilon_x$, where κ is the coupling parameter. In Table 2.6.1 we give steady-state emittances due to IBS for I = 1.5 A for bunch lengths σ_z = 2.5 mm and σ_z = 5.0 mm and for two couplings κ. At full coupling κ = 1, ε_x is minimized and is significantly less than 0.1 nm. The other couplings were chosen to give diffraction limited ε_y at 1-Å wavelength, ε_y = 8 pm. For these cases ε_x is somewhat larger than 0.1 nm. Note that the beam energy spread and bunch length for PEP-X parameters grow little under the influence of IBS. The last column in the table gives the Touschek lifetime T_l, calculated using the simulated dynamical momentum and horizontal apertures as well as the lattice functions in the entire ring. These calculations are based on the IBS determined, steady-state beam sizes. In the fully coupled cases, $T_l \sim$ 1.5-2 hours; in the diffraction limited cases $T_l \sim$ 0.5 hour. Finally, note that since both IBS and the Touschek effect depend on N and σ_z only as their ratio N/σ_z, I = 3.0 A, σ_z = 5.0 mm, emittances and lifetimes are identical to the ones when I = 1.5 A, σ_z = 2.5 mm.

Table 2.6.1: Steady-state emittance and Touschek lifetime at 1.5 A for two values of bunch length σ_z. In each case a full coupling result k = 1 and one which yields ε_y = 8 pm are given.

σ_z [mm]	κ	ε_x [nm-rad]	ε_y [nm-rad]	T_l [min]
2.5	1	0.082	0.082	81
2.5	0.045	0.18	0.0082	33
5.0	1	0.068	0.068	110
5.0	0.055	0.14	0.0079	42

Due to the very short lifetime, PEP-X will require a 3rd-harmonic rf cavity to lengthening the bunch to 5 mm. As discussed in Section 4.1.6, such a cavity introduces beam dynamics issues that require further study.

Even with a 5-mm bunch length, the beam lifetime at 1.5 A may need to be increased by increasing the vertical coupling. Frequent top-off injection will be required to maintain beam current constancy at the 1% level desired to maintain a constant power load on beam line optics in order to improve beam quality at user end stations. For example, assuming a 1-h lifetime at 1.5 A, 15 mA of beam current, or 110 nC of electron charge, would need to be replaced every 36 seconds. With the present limit of 8 nC per pulse from the present linac injector (Sec. 4.1.7), beam would need to be injected every 2 seconds to maintain 1% current constancy in this case (the time between injection pulses is proportional to the lifetime for this level of current constancy).

IBS and Touschek lifetime have been explored for 3.5- and 4-GeV beam energy [11]. The conclusion is that the emittance growth due to IBS for 1.5-A beam current essentially cancels the E^{-2} emittance reduction that would be expected by reducing the energy E for non-IBS-limited beams, and the net photon emission and brightness is reduced at these lower energies.

2.7 Collective Effects

The impedance of the rf cavities and vacuum chamber can drive single bunch and coupled-bunch instabilities in the ring. In this preliminary study we used some plausible assumptions regarding the impedance of the machine and considered the longitudinal microwave instability of the beam, an instability driven by coherent synchrotron radiation (CSR), and the transverse multibunch instability excited by a long-range resistive wall wakefield.

If the bunch rms length is chosen to be 2.5 mm, the threshold for the microwave instability is 2.5 A of total beam current. For a 5-mm rms bunch length, the threshold of the instability increases to about 8 A (Fig. 2.7.1).
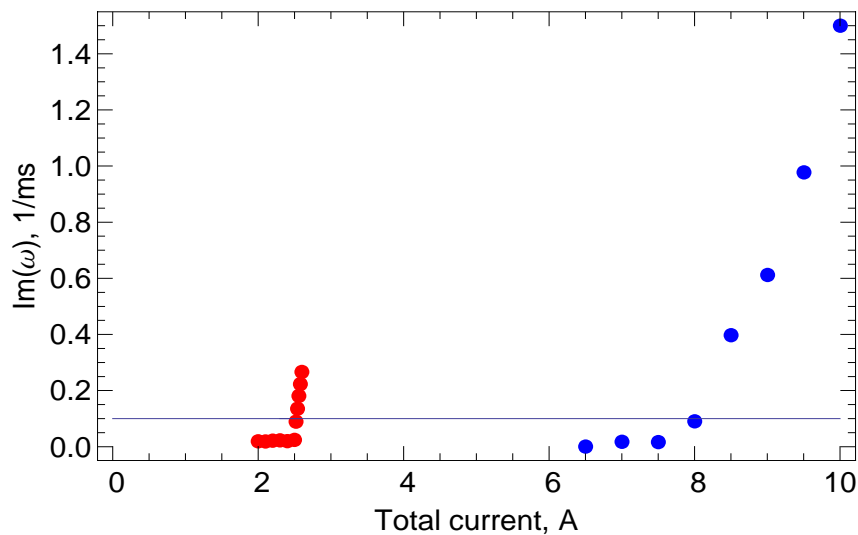
Figure 2.7.1: Thresholds for microwave instability for 2.5 (red dots) and 5 mm (blue dots) rms bunch length versus the total current in the ring. The horizontal line gives the value of the inverse synchrotron time 0.1 ms^{-1}.

We estimated the threshold peak current for the CSR-driven instability to be 154 A, corresponding to a total current of 1.5 A, assuming Gaussian bunches with a 2.5-mm rms bunch. We also found that the growth time of the transverse multibunch instability is equal to 0.38 ms (corresponding approximately to 50 revolutions) for this current and bunch length. This value does not change much for a 5-mm bunch length. Studies of this topic are on-going.

2.8 Fast Ion Instability

The ionization of residual gas by the electron beam generates positive that can be trapped by the electron beam and resonantly couple to the beam. Mutually driven transverse oscillations of an electron beam and ions can result in a fast transverse instability, called Fast Ion Instability (FII). The coupling force between the electron bunches and ions is inversely proportional to the cube of the transverse beam size. The estimated coupling force in PEP-X is about three orders of magnitude larger than that in B-factories (KEKB and PEP-II) due to PEP-X's ultra small beam emittance.

On the other hand, the ultra small beam size can drive partial ions unstable by overfocusing them. Therefore, fewer ions can be trapped with a smaller beam emittance. The trapped ions oscillate under the beam space charge force with a frequency depending on the local beam size. Since the beam size varies long the ring, the ion frequency spread along the ring provides additional landau damping.

The beam instability is simulated with a particle-in-cell program. The residual gas in the vacuum chamber is composed of monocular hydrogen (75%), carbon monoxide (14%), carbon dioxide (7%) and methane (less than 4%). We assume a constant pressure of 1 nTorr along the whole ring. The simulated growth time is shown in Table 2.8.1. A multi-bunch-train beam filling can reduce the number of trapped ions. Therefore, various beam filling patterns have been investigated. There is a faster instability in full coupling case because more ions can be trapped. With 8 bunch trains, there is a similar vertical growth time of 50 µs for 100%, 10% and 5% coupling due to the balanced effects of the coupling force, trapping condition and landau damping.

Table 2.8.1: Simulated beam growth rate with different coupling and beam filling patterns (bunch-train number×number of bunch per train). The total vacuum pressure is 1nTorr and the total beam current is 3.0 A.

Coupling	Number of bunches	Beam filling pattern	τ_x (µs)	τ_y (µs)
100%	3440	1×3440	42	12
	3440	8×430	105	40
10%	3440	1×3440	112	18
	3440	8×430	130	50
	3237	83×39	3300	294
	2988	83×36	3400	394
5%	3440	1×3440	116	24
	3440	8×430	133	58

The feedback response time of the present PEP-II feedback system is 500 μs. The growth time of 50 μs with a nominal bunch number 3440 is ten times faster than the feedback. A good vacuum of 0.1 nTorr is required for a 500 μs of FII growth time if the beam filling pattern of 8×430 is chosen. A compromise is to reduce the number of bunches to 3237 (83×39). This bunch-train filling pattern can significantly reduce the number of trapped ions and a growth time of 300 μs with 1 nTorr is achievable. In this case, a pressure of 0.5 nTorr would meet the feedback specifications.

2.9 Lattice Migration from PEP-II to PEP-X

The final PEP-X configuration could be reached in a series of four migration stages from PEP-II:

PEP-II: 1) the existing machine is setup for 4.5 GeV beam; 2) phase advance in four arcs 5, 7, 9, 11 is increased from 60º to 90º for a lower emittance.

PEP-2.1: 1) the IR low β straight is replaced with a FODO straight; 2) phase advance in arcs 1, 3 is increased from 60º to 90º and the special IR bending adjustment is removed; 3) 40 more sextupoles are installed in these arcs; 4) 90 m wiggler is installed in straight sections 2 and 6.

PEP-2.2: 1) DBA lattice is installed in arcs 1, 7; 2) photon beamlines are installed; 3) the HER RF cavities are relocated from straight 12 to straight 4.

PEP-X: 1) TME lattice is installed in arcs 3, 5, 9, 11; 2) lattice in straight sections is adjusted for better match to the TME arcs; 3) injection system is adjusted for maximum injection efficiency.

Parameters for the migration stages are listed in Table 2.9.1 shown for the beam energy of 4.5 GeV, rf voltage of 10 MV and the 90-m damping wiggler.

Table 2.9.1: Parameters for the lattice migration stages.

Migration stage	**PEP-II**	**PEP-2.1**	**PEP-2.2**	**PEP-X**
Betatron tune, x/y	28.529 / 29.61	31.19 / 32.23	47.105 / 32.13	86.23 / 36.14
Synchrotron tune	0.0458	0.0398	0.0324	0.0074
Momentum compaction	$1.69 \cdot 10^{-3}$	$1.33 \cdot 10^{-3}$	$8.95 \cdot 10^{-4}$	$4.72 \cdot 10^{-5}$
Emittance without IBS [nm]	7.4	0.41	0.32	0.094
RMS bunch length [mm]	3.9	13.8	11.0	2.5
RMS momentum spread	$3.0 \cdot 10^{-4}$	$1.18 \cdot 10^{-3}$	$1.14 \cdot 10^{-3}$	$1.12 \cdot 10^{-3}$
Damping time, $x/y/s$ [ms]	295 / 297 / 151	23 / 23 / 12	20 / 21 / 11	20 / 20 / 10
Natural chromaticity, x/y	-55.6 / -72.8	-46.1 / -41.0	-62.3 / -57.9	-132.7 / -72.8
Energy loss [MeV/turn]	0.22	2.84	3.16	3.27
Number of photon beamlines	2	2	32	32

2.10 Conclusion

The selection of topics studied in the chapter is based on the experience we have accumulated over many years working with SPEAR3, PEP-II, and ILC damping rings. The study shows that there is no show-stopper and the goals discussed at the beginning of this chapter are realistic and achievable. A summary of the main PEP-X parameters is shown in Table 2.10.1.

Many results of this study should be considered preliminary. For example, the broad-band wakefield, based on the LER of PEP-II, serves only as a rough approximation of the impedance model for the new machine. More investigations are necessary to firm up these calculations and to optimize the design.

Table: 2.10.1: PEP-X main parameters. Note that the emittances include the contribution from the intra-beam scattering assuming 5.5% coupling.

Energy [GeV]	4.5
Circumference [m]	2199.32
Horizontal emittance with IBS [nm-rad]	0.14
Vertical emittance with IBS [nm-rad]	0.0079
RMS bunch length [mm]	5.0
Total current [A]	1.5
Number of bunches	3200
Beam lifetime [minutes]	42

Our study does not yet show any evidence to exclude a possibility of storing 3-A beam current in the ring. Clearly, this current requirement will make the implementation of many technical systems more challenging and costly.

The study also provides us with many suggestions of how to improve the design:
- Introduce a third-harmonic cavity system to lengthen the bunch and therefore to further reduce the effect of intra-beam scattering and to mitigate the microwave instability
- A faster feedback system in the transverse planes may be necessary to control the fast-ion stability and multi-bunch instability due to the resistive-wall impedance
- Increase the momentum compaction factor to mitigate the microwave instability
- Increase the off-momentum dynamic aperture to increase lifetime

3. Photon Sources and Beam Lines

3.1 Photon Source Properties

The PEP-X ring will contain two double-bend achromat (DBA) arcs each of which includes 15 straights suitable for installation of insertion device (ID) source magnets. Each DBA arc is preceded by a 120-m long straight which can accommodate an additional very long ID. Four theoretical minimum emittance arcs and associated 120m long straights comprise the remainder of the ring. These latter arcs, which minimize the overall ring emittance, are not designed to serve as photon beam line source points. The DBA ID straights are 4.26m long which provides sufficient space to accommodate 3.5-m IDs after accounting for bellows and taper masks. The electron beam characteristics at the center of each DBA straight are listed in Table 3.1.1.

Table 3.1.1: Electron beam characteristics at the center of the 4.26-m ID straights in the DBA straights.

ε_x (nm-rad)	ε_y (nm-rad)	$\delta E/E$ (%)	β_x (m)	β_y (m)	σ_x (mm)	σ_y (mm)	σ_x' (mrad)	σ_y' (mrad)
0.144	0.0080	0.112	9.09	8.14	0.0362	0.0081	0.0040	0.0010

To illustrate the potential of PEP-X as a photon source, the calculated brightness and flux of several representative in-vacuum, hybrid, planar undulator magnets are presented in Figures 3.1.1 and 3.1.2, respectively. The magnetic parameters of these undulators, which are detailed in Table 3.1.2, are consistent with present commercially available magnet technology. Higher risk undulator designs utilizing cryogenically-cooled permanent magnets or superconducting magnets hold promise for higher performance but require some maturation of the associated technology. Thus the performance curves of Figures 3.1.1 and 3.1.2 offer conservative estimates of ID performance achievable with PEP-X. It should also be noted that the β_x and β_y values listed in Table 3.1.1 are not fully optimized for maximizing undulator brightness. Further refinement of the PEP-X lattice should result in more optimized β function values, yielding up to a two-fold increase in undulator brightness.
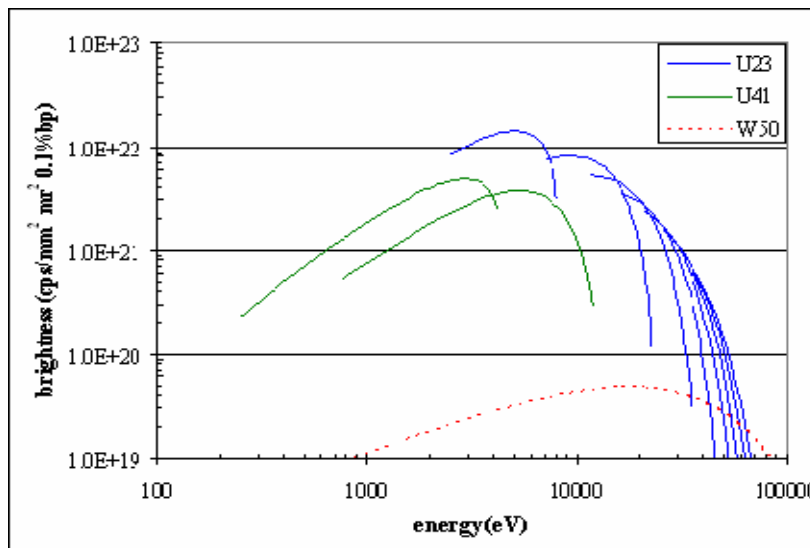
Figure 3.1.1: Calculated on-axis brightness of representative in vacuum insertion devices on PEP-X assuming the source and magnet parameters listed in Tables 3.1.1 and 3.1.2 and 1.5A stored current. Only the odd harmonic tuning curves are depicted for the two undulator sources U23 and U41. As noted in the text evolving magnet technologies and/or PEP-X lattice refinement could result in up to a two-fold brightness increase.
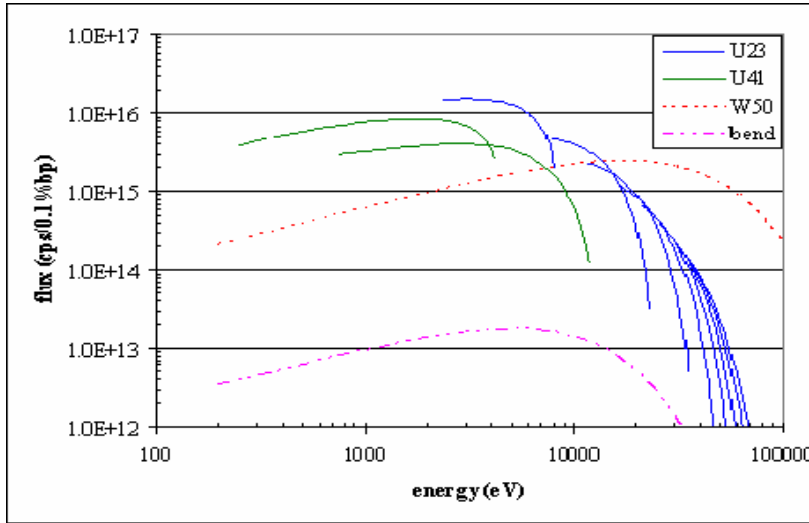
Figure 3.1.2: Calculated useful flux of representative sources on PEP-X assuming the source and magnet parameters listed in Tables 3.1.1 and 3.1.2 and 1.5 A stored current. The undulator curves represent the flux integrated over the central cone of the undulator emission spectra where only the odd harmonic tuning curves are depicted. The W50 wiggler and bend emission spectra are integrated over a 0.3-mrad horizontal by 0.1- mrad vertical acceptance.

Table 3.1.2: Representative source magnet characteristics. The minimum magnetic gap for the three in vacuum insertion devices is assumed to be 6.0 mm. Power values are for 4.5 GeV and 1.5 A.

	U23	U41	W50	bend
magnet	undulator	undulator	wiggler	dipole
period	23mm	41mm	50mm	n.a.
no. periods	150	85	70	n.a.
k_{max} or B	2.26	5.97	7.85	0.49T
Ecrit (keV)	14.2	21.0	22.6	6.6
power (kW)	74	166	191	0.29 kW/mrad
power dens (kW/mrad^2)	1038	884	784	1.6

The U23 undulator magnet characteristics are designed to provide continuous, odd harmonic tuning over a broad range of x-ray energies. The characteristics of this magnet are similar to several commercially produced in vacuum, hybrid, planar undulators recently installed on intermediate energy, third generation light sources worldwide including the BL12 undulator on SPEAR3. Demonstrated phase errors for such magnets are in the 1.5-2.0 degree range which results in nearly ideal brightness even when operating on high harmonic numbers.

U41 is a relatively long period, high-k undulator/wiggler as required to reach the carbon k-edge at 284 eV. Performance of an undulator operating in the softer x-ray regime can be enhanced by raising the minimum tunable energy (e.g. 1 keV) or degraded if the research program requires an elliptically polarized undulator. Since the characteristics of an undulator utilized for VUV or soft x-ray applications on PEP-X are likely to be tailored to meet the specific needs of the associated research program, the performance curves of the U41 undulator should be considered as only roughly indicative of VUV and soft x-ray undulator performance.

For applications which are not strictly brightness-limited and require photon energies in excess of approximately 20 keV, the pronounced roll off in U23 central-cone flux may pose an undesirable limitation. However, the PEP-X ring includes almost 100 m of damping wigglers

with 20-keV critical energy. A portion of this wiggler could be used as a source of higher energy x-rays. Alternatively, some standard straights in the DBA arcs could be utilized for wigglers. Characteristics of a representative 50-mm period, in vacuum wiggler in a DBA straight are listed in Table 3.1.2 and its performance is depicted in Figures 3.1.1 and 3.1.2. The on-axis brightness of this wiggler falls well short of the U23, but the useful flux, defined here as the flux integrated over a 0.3-mrad horizontal by 0.1-mrad vertical acceptance, exceeds that of the U23 for energies in excess of 15 keV. As discussed in section 4.2, power deposited on the photon optics from such a source poses a significant engineering challenge.

For completeness, Table 3.1.2 lists the characteristics of a DBA dipole source while Figure 3.1.2 depicts the useful flux radiated by the dipole source. This relatively modest performance source is not envisioned to comprise a significant fraction of the PEP-X beam line capacity owing to competition with higher performance ID beam lines for experimental hall floor space.

3.2 Beam Line and Experimental Hall Layout

The extraordinary power density radiated by a PEP-X ID poses significant challenges for beam line component and optics design. Rather than rely upon speculative improvements in mask and optics power handling capabilities, the proof of principle layout of PEP-X beam lines discussed here assumes existing limitations on component thermal performance. Consequently, as detailed in Section 4.2, the preliminary beam line layouts employ long drift lengths to reduce power densities and aggressive beam aperturing and filtering to minimize total power deposited in key optical components. This conservative approach ensures the feasibility of the beam line design but it may tend to over estimate the cost and space requirements for the beam line components.

Limiting the power density intercepted by beam line front end components to manageable levels for existing technology results in placing front ends approximately 50-60 m from the source. Radiation shielding considerations demand that the front end and associated radiation stoppers be located inside the storage ring concrete shield wall. To accommodate these components and a low-pass filter mirror inside the storage ring shielding, the beam pipe penetration through the shield wall out to the experimental hall is located 70 m from the source (Figure 3.2.1). While this renders part of the beam line inaccessible during storage ring operations, it affords significant advantages from a radiation shielding perspective. In particular, locating the low-pass mirror inside the ring shielding substantially simplifies the shielding requirements for Compton scattered synchrotron radiation and laterally scattered gas Bremsstrahlung.

The beam exits the ring shielding into an 11-m-long first optics enclosure (FOE). The FOE provides sufficient length to accommodate all necessary grazing-incidence power masks and slits, the monochromator, experimental hutch stoppers, and Bremsstrahlung shielding. Focusing mirrors follow the FOE in the space upstream of experimental hutches. The layout of Figure 3.2.1 assumes tandem hutches each of which is 4m x 8m. Beam line control stations are envisioned to be located downstream of the experimental hutches.

The experimental hall layout of Figure 3.2.1 depicts a standard beam line length of 110 m to the back experimental station. This layout provides adequate room for typical focusing optics. Note, however, every fifth beam line is allocated 140 m to accommodate beam line configurations that require additional length such as highly demagnifying optics. Moreover, several beam lines situated towards the downstream end of the DBA arc could be extended substantially with the elimination of the downstream lab and office module. The most upstream beam line in each

experimental hall utilizes an ID situated in the 120 m-long straight. Depending on where the ID is positioned in the long straight, the experimental hall as depicted in Figure 3.2.1 can accommodate up to 250 m of total beam line length. By extending the experimental hall along the axis of the 120m straight an ultra long beam line in excess of 500 m is feasible for the arc 1 hall (see Figure ES.1).
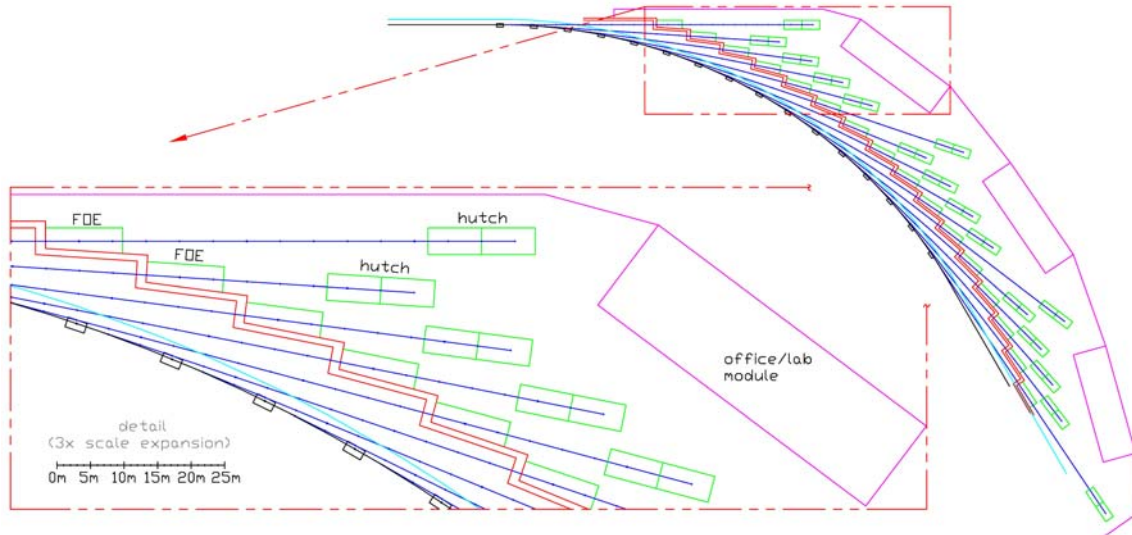
Figure 3.2.1: The preliminary layout of one of the two experimental halls. The detailed inset at the lower left provides a 3x scale expansion of approximately one third of the hall including one 140m beam line, four 110m beam lines, and one 15m x 50m office/lab module. The ring concrete shield wall is the red saw tooth structure. The ~3.5m x 11m FOE are depicted in green as are tandem 4m x 8m experimental hutches located at the end of each beam line.

Co-located with each cluster of five beam lines is an approximately 8000 square foot lab and office module. Each module provides space for two 600 square foot labs as well as offices and small conference rooms for approximately 40 light source and beam line staff. Each experimental hall includes three such modules. The experimental floor of each hall comprises approximately 100,000 square feet of column-free high bay while the storage ring shielding encloses another 25,000 square feet per arc resulting in a total building area of approximately 150,000 square feet.

3.3 Soft X-ray FELs

Studies indicate that the radiation from a 50-100 m undulator whose first harmonic is tuned to < ~400 eV would be enhanced by one to two orders of magnitude by the SASE FEL process acting with the stored beam[12]. For the 3.3-nm (379 eV) case shown in Figure 3.3.1, the peak bunch current must be 270 Apk (~1 mA in a 10-ps rms bunch) and the electron beam must be fully coupled to minimize emittance growth from intrabeam scattering (Sec. 2.6). The SASE process does not reach saturation; instead a partial lasing equilibrium is reached between the SASE-induced energy spread and bunch lengthening (which reduces peak current) and the FEL gain (Fig. 3.3.1).   Such an FEL undulator would provide a significant fraction of the damping needed to reach low emittance, reducing the total length of other dedicated damping wigglers.
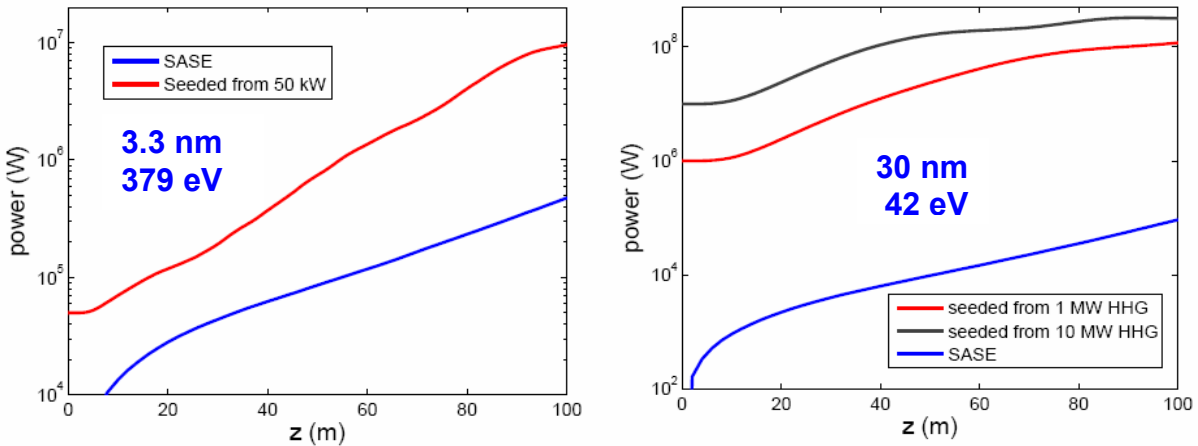
Figure 3.3.1: Simulations of the power evolution of a 3.3-nm SASE FEL (left) and 30-nm FEL (right) using an equilibrium energy spread (1.26 x 10^-3) and 270-Apk current in PEP-X having an emittance of 0.07 nm-rad (blue). The undulator for the 3.2-nm case has a 5-cm period and a 1-T peak field. Seeded-FEL simulations are shown in red and black.

The drawback to the partial lasing ID is the very large spontaneous radiation power that would emitted with a 1.5-A stored beam (~4 MW, ~26 MW/mrad^2). This power density would result in ~20 kW into a 30 μrad x 30 μrad beam line acceptance aperture, over a factor of 10 higher than present monochromator technology permits. The total beam current, and the average brightness for other users, would therefore have to be reduced to ~150 mA in ~150 bunches for operating in this mode. An alternative is to periodically switch some fraction of the electron beam into an FEL bypass with a duty cycle that is tolerable for both the FEL beam line optics and other users. Laser seeding at the radiated wavelength could also be used to induce periodic lasing in a shorter undulator with a seeding repetition rate in the kHz range (Figs 3.3.1 and 3.3.2). At present, laser seeding sources having sufficient power only exist for wavelengths >~10 nm.

Using an injector with a high brightness gun, similar to that used for the LCLS FELs, high peak power saturated-FEL pulses over the wavelength range of 1.5 to 50 nm, having full transverse coherence and pulse lengths between 50 and 1000 fs, could be produced in a 50 to 100-m undulator [13]. Such a high-brightness electron bunch could be injected in a gap between the stored electron bunches using a very fast on-axis injection kicker [8]. The repetition rate would be the same as that of the injector. The high-brightness, ultra-short electron bunch would have to be transported to the undulator through a suitable isochronous lattice. Studies show that coherent synchrotron radiation (CSR) effects will disrupt bunch quality if the transport optics contains too many bending magnets, as would be the case if attempting to inject such a bunch from the LCLS injector located in the main SLAC linac vault [14].

While it is as yet unclear whether these or other FEL ideas are practical for PEP-X operation, they will continue to be considered in future PEP-X studies.

3.4 RF Undulators

PEP-X could benefit from the use of rf undulators, presently under development at SLAC [15]. These devices enable fast polarization switching (with kHz repetition rates), variable undulator period control, and the possibility of fast on-off switching for SASE FELs that would greatly

reduce the total radiated power from the stored beam, as discussed in Section 3.3. These devices use high power rf in a waveguide to produce a periodic field using technology based on the recent development of a 500 MW X-band rf source for the Next Linear Collider at SLAC combined with advances in over-moded rf components.

Two rf undulator configurations presently being investigated have a K of ~1 in the soft x-ray regime: 1) a "pearl string resonator", consisting of a series of spherical cavities, and 2) a cylindrical waveguide resonator. Each operate at S-band rf frequencies, but could support shorter period lengths if operated at X-band or W-band frequencies. The rf power repetition rate is expected to be in the kHz range.

4. PEP-X Implementation

4.1 Accelerator Systems

With the exception of the PEP-II rf system, much of the existing utility systems, and the majority of the PEP-II tunnel sections, the PEP-X accelerator systems will either be new or reworked from existing components (e.g. some magnets). PEP-X accelerator system implementations are summarized in the following sections.

4.1.1 Magnets and Supports

The PEP-X magnets will be a combination of newly constructed and reworked PEP-II magnets. Reworked magnets, comprising ~25% of all magnets for PEP-X result in considerable cost savings. The remaining magnets will be constructed from new materials using proven design expertise from SLAC with use of outside construction vendors. Very high field quality will be required for these magnets to maintain dynamic aperture in the ring.

Magnet support girders will be designed for maximum rigidity and stability in order to minimize orbit motion. The lowest magnet girder vibration mode frequency will be >25 Hz. Magnets and support girders will be thermally stabilized to the order of 0.1^{o}C to reduce thermally induced motion to the order of 1 μm vertically.

The complement of magnet types and associated power supplies are listed in Table 4.1.1. In addition, 360 to 500 horizontal correctors, and almost as many vertical correctors, are required. The exact number and locations of the correctors will be determined by future orbit correction studies. In many cases the horizontal and vertical correctors can share the same iron core. A subset of correctors will be used for fast orbit feedback, requiring ~1 kHz bandwidth.

4.1.2 Magnet Power Supplies

PEP-X will be equipped with new magnet power supplies. Some power supply components from PEP-II will be reused, but it is also expected the power supply technology will be superior and entirely digitally controlled in the future. In general, magnet power supplies will need to be very stable (1-30 ppm, depending on magnet type), have very low ripple to maximize high-frequency orbit stability, and have a high operational reliability and maintainability. The complement of lattice magnet power supplies are listed in Table 4.1.1.

Not included in Table 4.1.1 are the 750 to 900 bipolar orbit corrector power supplies, whose exact number will be determined by future orbit correction studies. Many of these supplies will be used for fast orbit feedback, requiring a bandwidth > 1 kHz. Corrector setpoint resolution must be sufficiently high to avoid generating orbit disturbances as a result of setpoint quantization noise. In modern light sources, 18-bit digital-to-analog converters are used in the power supply controllers for 1-mrad correctors to meet this requirement. In PEP-X, even higher setpoint resolution, or less corrector range, will be needed to reduce induced orbit noise well below 10% of the electron beam dimensions.

Also not included in Table 4.1.1 are many miscellaneous power supplies that will be used for quadrupole modulation, skew quadrupoles, and other special magnets.

Table 4.1.1: Lattice magnets and power supplies (PS) for PEP-X, not including orbit correctors injection magnets, and other special magnets.

	Magnet families	Number of magnets	Number of PS
DBA arc dipoles	BEND	64	2
TME arc dipoles	B, BM	136	4
	Total dipole:	200	6
DBA arc quadrupoles	QFCZ	64	2
	QFZ	60	60
	QDZ	60	60
	QFAZ	4	4
	QDAZ	4	4
TME arc quadrupoles	QF	256	4
	QD	256	4
	QFM1	8	4
	QDM1	8	4
Straight section quadrupoles	QDS1D	4	4
	QFS1D	4	4
	QDSE	20	2
	QFSE	16	2
	QDS1	4	1
	QFS1	4	1
	QDS2	8	1
	QFS2	8	1
	QDS3	8	1
	QFS3	8	1
	QDSEW	5	1
	QFSEW	4	1
	QDS1W	2	1
	QFS1W	2	1
	QDS2W	2	1
	QFS2W	2	1
	QDS3W	2	1
	QFS3W	2	1
	QDS1I	2	1
	QFS1I	2	1
	QDS2I	2	1
	QFOI	2	1
	QDOI	2	1
	QFI	2	1
	QDI	2	1
	Total quadrupole:	839	179
DBA arc sextupoles	SFI	32	2
	SDI	64	4
TME arc sextupoles	SF	128	8
	SD	256	16
	Total sextupole:	480	30

4.1.3 Damping Wigglers

The ~90 m of damping wigglers (Sec. 2.2) will consist of 18 or more new magnets whose individual length will be 4-5 meters. The damping wigglers will be located in one or two long straight sections. The radiated power and power density for a 5-m wiggler with a 10-cm period and 1.5-T peak field are 220 kW and 500 kW/mrad^2, which must be accommodated by a suitable system of power absorbers. The accumulation of on-axis photon power for a series of in-line damping wiggler sections in a straight section presents a significant challenge for the design of the photon absorbing system. While this geometry has been adopted for the PETRA-III damping wigglers [16], the power levels are an order of magnitude large for PEP-X. Future R&D will be devoted to solving this problem for the in-line wigglers. If a workable solution is not found, it will be necessary to cant each wiggler section and the beam orbit by 3-4 mrad at the expense of increased emittance in order to direct the radiated power from each section to a specific photon absorber. The power density at each photon absorber must be reduced to ~5-10 W/mm^2, assuming present absorber technology is used, through a combination of inclination angle of the absorber with respect to the photon beam and its distance from the source. For example, the power from a 5-m wiggler section could be handled by an absorber having a 1.5-degree grazing angle of incidence, located 50 meters away.   The length of this absorber exceeds 1 m to accommodate the photon beam footprint assuming reasonable (mis)steering envelope. As discussed in Section 3.1 shorter damping wiggler sections might also be located in DBA arc straight sections to serve as hard x-ray photon sources for beam lines.

Damping wigglers will most likely use permanent magnet rather than electromagnet technology to reduce operational power, although future superconducting technology may be considered. Radiation-damage resistant permanent magnet material will be used to maintain very high magnet field quality.

Fabricating the wiggler magnets could be an excellent project for international collaboration. For example, the damping wigglers for PETRA III were designed and built in the BINP laboratory in Novosibirsk, Russia [16], and were delivered on time and on a reduced budget compared to local industrial vendor bids for the DESY laboratory.

4.1.4 Vacuum System

All new vacuum chambers will be needed in the PEP-X arcs in order to accommodate the new magnet lattice and aperture requirements. It is likely that some PEP-II chambers could be reused for the straight sections.

The new vacuum chambers will be a combination of aluminum and copper depending on synchrotron radiation power handling requirements. Discrete absorbers, most likely fabricated from Glidcop™, or a material having similar properties, will be used in antechambers for high photon power densities. Special attention must be paid to maintaining a low vacuum chamber impedance by minimizing chamber discontinuities and component cavities that can trap higher order rf modes (HOMs) induced by the short electron bunches. The beam duct aperture dimensions will be an optimized trade-off between large size to reduce resistive wall impedance and small size to reduce magnet apertures (and thus reduce material and power costs) and the need for significantly tapered ID chamber transitions, which have relatively high impedance. The first estimate for the nominal magnet girder beam duct aperture is 75-mm wide by 25-mm tall.

PEP-X will be equipped with ~800 beam position monitor modules, with the actual number and locations dependent on future orbit correction analyses. BPM buttons, most likely having a diameter of 6-8 mm, and feed-throughs, as well as rf-shielded bellows, will be designed to minimize trapped HOMs and related heating. The chambers will have a sufficient water cooling system to minimize chamber motion due to beam heating at critical locations (e.g. BPM sites) that could affect beam orbit motion and photon beam stability. Highly stable BPM modules, possibly supported by thermally stable Invar, will be located upstream and downstream of insertion devices and will be used in a feedback system to maintain ultra-high photon beam stability. The vacuum chambers for PEP-II, whose accelerator rings operated with 2-3 A, were designed and built at SLAC, which has the expertise to design and build the PEP-X chambers and associated components.

Vacuum pumping will be provided by a combination of localized ion and TSP pumps together with the possibility of distributed NEG pumps. While it is expected that most of the PEP-II ion pumps can be reused, new ion, TSP and NEG pumps will be required. It is probable that small-gap ID vacuum chambers will be NEG-coated to provide sufficient pumping in those locations. A combination of new and reused vacuum pump power supplies will be used.

4.1.5   RF system

The present PEP-II RF system is one of the best in the world and is adequate to operate PEP-X with high current at 4.5 GeV. There are 15 full stations available, each station powering two or four single-cell, mode-damped cavities. Each station is equipped with a single 1.2-1.6 MW, 476-MHz CW klystron and associated high-voltage power supply and low-level rf controls [17]. Characteristics of the RF cavities are shown in Table 4.1.2.

Table 4.1.2: Properties of the PEP-II mode-damped rf cavity.

Frequency	476 MHz
Shunt impedence (R_s)	3.5 MΩ
Coupling factor without beam (β)	3.9
Unloaded Q	~30,000
Maximum power into cavity	500 kW

Eight or more PEP rf stations, each driving two rf cavities, will reliably provide power for any of the ring implementation scenarios outlined in Section 2.9 (PEP 2.1, 2.2, or X) operating at 1.5-A beam current. The klystron powers, cavity reflected energies, and electric fields at rf windows will all be well below their limits. Longitudinal stability should not be a problem, as cavity detuning, current, and beam impedance will all be less than for operation of PEP-II.

For PEP-X, two or three rf stations will need to be relocated from PEP Region 12 to Region 8, and waveguides in Region 4 will need to be modified. A new low level rf system will be needed for better control of rf parameters.

Operation of up to 3-A beam current is feasible, but it would be challenging. Twelve rf stations should provide enough power, but the cavity coupling boxes would need to be modified to efficiently couple this power to the cavities without causing arcs at the rf windows. Low-order longitudinal modes will tend to be unstable at these currents, likely requiring new longitudinal

feedback filter designs. These problems should be soluble, but will require extensive simulations and cavity tests.

These cavities have been conditioned to ~750 kV, but tend to arc occasionally at these levels. To achieve high reliability for PEP-X, we plan to operate them at 600 kV maximum. A higher reliable operating voltage might be reached if studies can reveal the source and solution of the arcing problem.

4.1.6 Bunch-Lengthening Cavity System

In order to increase beam lifetime and to reduce the heat load on the vacuum system components, it is of benefit to keep the bunches in the ring relatively long. This requirement conflicts with the low-emittance PEP-X lattice design which has an inherently small momentum compaction and correspondingly short bunches for any rf voltage that is sufficiently high to give good longitudinal acceptance. This dilemma can be addressed by introducing higher-harmonic rf cavities phased in such a way as to lower the slope of the rf voltage at the synchronous phase—ideally to zero. In this way the bunch length can roughly be doubled for the same energy acceptance of the ring. This is optimally done at the 3rd rf harmonic.

The 3rd harmonic rf voltage does not deliver energy to the beam and can in fact be provided by passive cavities excited by the beam current. The cavities are detuned (positive, or inductive) for the induced rf voltage to have the desired phase. The amplitude is controlled by the amount of detuning (frequency offset). Superconducting cavities are ideal for this application since the phase of the voltage with respect to the beam is 90° practically independent of the amount of detuning, and, due to the high shunt impedance, the desired voltage can be reached even at small beam current. Examples are cavities built for SLS and ELETTRA (Super3HC) [18] and BESSY (based on a Cornell design) [19]. Room temperature cavities have been used for ALS [20].

For PEP-X, the optimal voltage of the 3rd harmonic rf is about 30% of the fundamental rf voltage, about 3 MV. In fact, 2.5 MV are sufficient to double the bunch length; this could be provided by 3 cryomodules of the Super3HC-type 2-cell cavity or by 5 modules of the BESSY-type cavity. The cryogenic power needed is on the order of 200 W at 4.4 K, to be compared with about 1 kW of cryo power installed in the Research Yard at SLAC. Table 4.1.3 summarizes the parameters for a BESSY-type system.

Table 4.1.3: Parameters for a 3rd harmonic bunch-lengthening cavity system.

Parameter	Value	Unit
Voltage	2.5	MV
Frequency	1428	MHz
# cavities	5	(BESSY/Cornell type)
Shunt impedance	10^{10}	Ω
Q	2×10^8	
R/Q	50	Ω
P/cavity (dynamic)	12.5	W
P$_{cryo}$, total	≈125	W (static & dynamic)
Detuning	215	kHz

Beam dynamics issues associated with the use of 3rd harmonic cavities included detuning to the Robinson-unstable side of the rf frequency, which, given the rather high beam current in PEP-X,

could lead to beam stability issues. Because of the cancellation of the slopes of the fundamental and 3rd-harmonic rf voltages the bunch length may become very sensitive to phase transients induced by the ion-clearing gap [20]. It is conceivable that some of these issues could be addressed by a more complex active system. We plan to study these issues in detail analytically and in simulations.

4.1.7 Injection System

Precluding its use for other projects at SLAC, the electron injection system for PEP-X will be the same as that used for the PEP-II HER. The injector includes a damping ring, 12-GeV linac and transport line and is fully capable of injecting adequate beam into PEP-X with very few improvements, if any, needed for reliability. The injection charge capability is up to 5×10^{10} electrons (8 nC) per pulse at 120 Hz. As discussed in Section 2.6, the short PEP-X lifetime requires frequent top-off injection to maintain beam current constancy at the 1% level. It is expected that ~8 nC would need to be injected every 1-2 seconds (18-36 W injected beam power) for beam lifetimes of 30-60 minutes at 1.5 A, and that this charge would be distributed in ~12 buckets.

In order to minimize the impact of 1-Hz injection on user beam quality, the injection kicker bump will be compensated to a high degree to reduce the stored beam orbit transient and user data acquisition injection-gating and synchronizing techniques will be developed. The full width of the existing PEP half-sine kicker pulses is ~0.4 μs and therefore affects only ~6% of the stored bunches in PEP, so even kicker-induced stored beam orbit transients on the order of ten times the beam size (on the order of 100 μm rms) would have an effective integrated amplitude <10% of the beam size in if data is averaged over ~6 revolution periods (~45 μs) or more. Data gating would be required for experiments having shorter integration periods.

The present plan is to retain the PEP-II vertical injection scheme with its septum and kicker magnets. If it is determined that vertical injection is not acceptable, a horizontal injection scheme will be adopted. This will require new septum and kicker magnet designs, as well as a rerouting the injection transport line.

Use of the existing injector for PEP-X may conflict with future SLAC projects (e.g. FACET and/or LCLS-U3). In this case, a new 4.5-GeV linac for PEP-X would be constructed using available spare parts (including 3-m copper accelerating sections and klystrons). New controls and klystron modulators would be needed. Such an injector could be installed in IR-8 of PEP-X, making it independent of the other linac programs. With a new low-emittance rf gun, there would be no need for a damping ring to achieve the requisite injection beam properties. The linac would provide 10 to 20 bunches per pulse, with ~10^9 electrons in each bunch (0.16 nC, or 0.02 mA of beam current, per injected bunch) at up to 120-Hz repetition rate.

4.1.8 Instrumentation, Control and Feedback Systems

The PEP-II computer control system will need to be replaced for PEP-X. It is expected that a widely used control system standard, such as the EPICS control system toolbox, will be adopted along with many application and driver software packages that will have been developed by the controls community. State-of-the art hardware interface technology will be used. It is expected that controls will be distributed around the PEP-X ring in the support buildings associated with each of the six long straight sections. It is likely that, as much as possible, Ethernet LANs or the equivalent will be configured to communicate with distributed controllers embedded in

individual processing and control components, thereby minimizing the control system cable plant. Device control and readback data rates will be sufficient to achieve desired component performance, ranging from rates on the order of 1 Hz for slow devices (e.g. temperature and pressure monitors) to many kHz (e.g. for hundreds of digitally controlled orbit feedback power supplies and BPM processors), and MHz for wideband devices. The technology that should be used to achieve these very high data rates in a distributed network will be investigated in future studies.

PEP-X will require electron and photon beam monitoring instrumentation that surpasses the present state of the art for storage ring light sources. Instrumentation requirements include BPM processors that can achieve sub-micron resolution in a few hundred Hertz bandwidth as well as first-turn and turn-by-turn orbit measurements (perhaps of individual bunches or localized bunch trains), a quadrupole modulation system that can be used to establish BPM electrical centers with respect to quadrupole magnetic centers, beam loss monitors to maximize injection capture efficiency, transverse profile monitors that can resolve the micron-level electron beam size, a high-resolution bunch current monitor (which will aid automated top-off injection), a bunch purity monitor for photon timing mode experiments, a precision total current monitor (DCCT), a high resolution tune monitoring system, and other diagnostics. Many systems having performance specifications at or near the PEP-X requirements are already available. Laser wire technology, such as that being implemented at PETRA III [21], might be employed to measure the very small electron beam transverse dimensions in place of a synchrotron radiation monitor, which is likely to have insufficient, diffraction-limited beam size resolution. Photon BPMs in the beam lines will be used to improve photon beam stability before and after optical components.

As discussed in Section 2.5, advanced orbit and beam line feedback systems will be needed to achieve the requisite level of electron and photon beam stability (<10% of photon beam dimensions) in PEP-X. An integrated effort from the accelerator and beam line designers will be needed to maintain stability integrity in all aspects of hardware and control system design. It is likely that high-resolution (~100 nm or better) mechanical motion/position survey sensors will be needed for critical components in the accelerator (e.g. user BPMs) and beam line (e.g. optical components, small apertures and collimators, etc). Some of these devices may require cutting-edge technology (e.g. "telescope technology" such as the laser-Doppler stabilization system used for atomic force microscopes and the X-ray Nanoprobe at the APS [22]). Maintaining the beam pointing and position stability at user experimental stations located >100 m from the photon source will is an engineering challenge. BPMs will be located near sextupoles, as well as quadrupoles, in order to maintain precise orbit centering in them to maximize dynamic aperture.

High frequency electron bunch motion, driven by accelerator transverse and longitudinal impedances will be controlled with bunch-bunch feedback systems. Feedback kicker bandwidth must be at least half of the 476-MHz rf frequency to affect bunches separated by 2.1 ns. Longitudinal instability caused by rf voltage phase and amplitude noise, including that caused by ripple in the high voltage power supply at harmonics of 60 Hz, must be controlled with a combination of the low-level rf and longitudinal multibunch feedback systems. It is expected that the action of a third harmonic bunch lengthening cavity may complicate fast rf and longitudinal feedback system performance, requiring further development of those systems.

4.1.9 Machine and Personnel Protection Systems

Protection interlocks for accelerator vacuum and magnets will be configured using robust programmable logic controller (PLC) technology, a technology that is bound to evolve significantly in the next decade. The usual array of vacuum pressure sensors, component temperature monitors, water flow sensors, component position detectors, etc., will be incorporated in the machine protection interlock to guard against component and system damage. A fast orbit interlock, which protects parts of the vacuum chamber and beam line components from mis-steered high-power photon beams, will be required to maintain the electron beam orbit within a tight channel when beam current exceeds an inherently safe level for mis-steering. Beam loss monitors around the ring may be interlocked to protect against excessive injection losses that could damage permanent magnet IDs and other sensitive components.

Personnel protection systems include those for accessing the ring tunnel and beam line experimental stations. These fully redundant interlocks will be configured using highly reliable and secure PLC systems designed for such use. A beam containment system will also be configured in this way, employing safety-rated beam loss monitors, linac and transport line current monitors, beam shut-off ion chambers, and other devices designed to maintain radiation levels within safe limits determined by the radiation shielding implementation.

4.1.10 RF Beam Manipulation Components

PEP-X may contain special accelerator components, such as transverse crab cavities or other rf components, together with their high-power rf power sources, for bunch phase space manipulation [8,9]. In one novel implementation, rf deflecting cavities might be used to exchange longitudinal and vertical electron beam emittances to produce very short bunches (<100 fs) at the expense of large vertical beam size (several millimeters) [23].

These rf components and systems will require an extensive R&D and design effort.

4.1.11 Cable Plant

It is expected that much of the aging PEP-II cable plant will need to be replaced for PEP-X.

4.1.12 Utilities

The AC power, water cooling, and support buildings exist for PEP-X, but will most likely require refurbishment in the future. The air-handling in the tunnel may need to be reworked and upgraded to handle tighter tolerances on air temperature stability needed.

4.1.13 Accelerator Tunnel and Shielding

The PEP-II accelerator tunnel must be modified in two arcs to accommodate the DBA lattice and associated photon beam lines (Figs. ES.1 and 3.2.1). The tunnel in these two arcs must be rebuilt to provide the ratchet wall shielding geometry needed for photon beam line penetrations as well as to provide an aisle on the inner side of the accelerator wide enough (>~1.5 m) for equipment access and installation in the DBA straight sections. On the order of 2×10^5 yds^3 of earth must be excavated in the arc 1 area to expose the accelerator tunnel and provide the area needed for the experimental hall described in Section 3.2. Far less excavation is required in arc 7.

Ratchet wall shielding thickness will be determined by the calculated neutron and gamma radiation doses caused by both the stored and electron beams. It is likely that the 20-40 W injected beam will be the predominant factor in this determination. It is estimated the lateral

shielding walls will be ~1-m thick, and the transverse walls will be ~1.5-m thick. Polyethylene will be used to shield neutrons, and additional lead and/or steel will be used for localized shielding as needed. An alternative shielding implementation that will be considered in the future is to replace some of the excavated earth to provide some fraction of radiation shielding. Earth has a density that is ~70% that of heavy concrete, so ~7 ft of earth would provide the equivalent of 5 ft of concrete shielding.   Much further analysis is required from the Radiation Physics Department to establish actual shielding requirements.

Further analysis is needed to determine if the concrete tunnel floor in the DBA arcs needs to be rebuilt for additional stability. A significant engineering task is to determine how or if the accelerator floor will connect with the experimental hall floor to achieve maximum stability of each beam line with respect to the electron orbit in the associated photon source magnet.

The accelerator tunnel in the four TME arcs may require refurbishment to control water seepage and other imperfections.

4.1.14 Facility Preservation

The successful reuse of equipment from PEP-II will depend on proper maintenance over the next decade. Vacuum chambers will be vented to dry nitrogen, water cooling channels for vacuum chambers and magnet conductors will be drained and blown dry, and a program of preventive maintenance and/or safe storage will be instigated for all components of value, including power supplies, instrumentation and control components, utility infrastructure and other accelerator components.

4.2 Photon Beam Line Systems

The preservation of photon beam emittance, coherence and stability in the presence of the unprecedented beam power of PEP-X poses a significant challenge for beam line design. While it is reasonable to assume improvements relative to the current state of the art of beam line component and optics technology, this report outlines a conservative, proof of principle beam line design respecting the constraints imposed by existing technology. Consequently, preliminary beam line layouts utilize long drift lengths to reduce power densities to manageable levels and aggressive beam aperturing and filtering to minimize the power deposited in key optical components. Nonetheless, optics designs based on current technology cannot preserve fully the extraordinary emittance of the PEP-X source. Emittance preservation is likely to be enhanced as x-ray optics technology evolves.

4.2.1   High Power Beam Lines

As detailed in Table 3.1.2, the U23 undulator develops the greatest power density of the representative ID sources. Power density represents a key constraint in beam line design as it defines the minimum distance between source and first power masks. As demonstrated shortly, once properly apertured and filtered, the optics can manage the remaining thermal load with relatively modest power-induced degradation of the beam emittance. The higher total power though lower power density of the longer period ID, such as W50, alter the beam line design problem. These inherently lower-brightness ID beam lines reduce the emphasis on emittance preservation, but the optics must cope with greater total power to extract the maximum performance from the source. Since these sources represent a minority application on a low emittance ring such as PEP-X and a successful undulator beam line design solution can be

applied to a wiggler by reducing the beam line acceptance (at the price of reduced flux), our proof-of-principle design focuses on a U23 undulator beam line.

The peak power density of U23 with PEP-X at 4.5 GeV/1.5 A is 1038 kW/mrad^2 at k_{max} as listed in Table 3.1.2. Typically, intensively water-cooled Glidcop masks can tolerate 5-10 W/mm^2 steady state power deposition over large areas where the larger value can be sustained only if the mask surface can be profiled to expand the power footprint (e.g., a "crenelated" mask surface divides the power footprint into displaced alternating power stripes, resulting in a lower surface average power density). If one assumes the smaller 5 W/mm^2 limit and a 0.75°-1.0° beam incident angle, then the first masks that intercept the U23 peak power density must be at least 52-60 m from the source. Figure 4.2.1 plots the U23 beam horizontal and vertical power density variation with observation angle. At 60m from the source the beam half width at 10% power density is 16.5 mm horizontal by 9.0 mm vertical. Assuming rather stringent ±0.1 mrad beam steering tolerance increases this 10% power density half envelope to 22.5 mm by 15.0 mm. At 1.0° incident angle 1.3 m of mask is required to intercept 22.5 mm of beam. This is technologically feasible, particularly if distributed over several mask assemblies.

It should be noted that a ±0.1 mrad maximum steering envelope does not provide much steering tolerance for stored beam configuration development. The steering tolerance can be expanded at reduced stored current by employing larger acceptance, thermally de-rated masks upstream of the full power rated front end components. These de-rated masks could consist of relatively low-cost refractory metal collimators with thermal sensors for machine protection and/or short water-cooled Glidcop masks with steeper beam intercept angles.
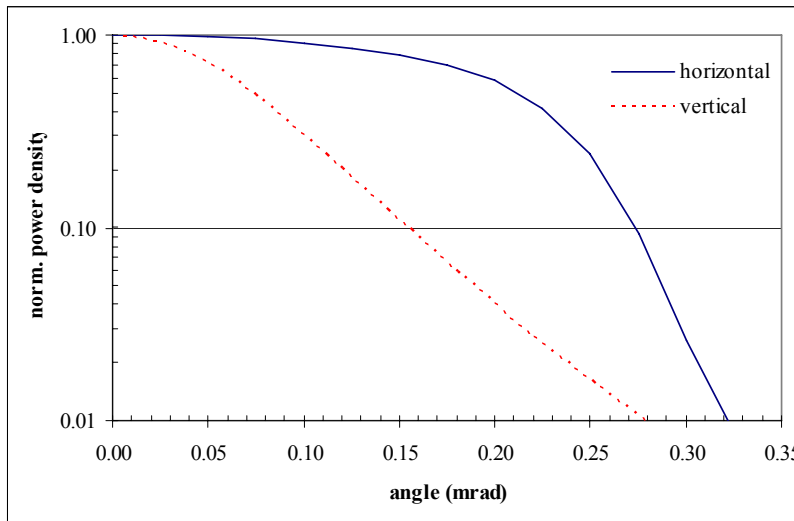
Figure 4.2.1: The U23 normalized power density at k_{max} as a function of horizontal and vertical observation angle for the ring and undulator parameters tabulated in Section 3.1.

It is advantageous to intercept and discard as much waste power in the front end masks as possible in order to minimize the power on downstream masks and optics. Utilizing apertures to limit the beam line acceptance to 3σ′, where σ′ is the effective rms angular width of the undulator central cone, transmits almost 90% of the central cone flux. The undulator effective central-cone opening angle as a function of photon energy is listed in Table 4.2.1. Inspection of this table indicates a 30 μrad by 30 μrad acceptance is adequate for a broad range of x-ray energies. For higher energy applications a more restrictive 20 μrad by 20 μrad acceptance is sufficient. Figure

4.2.2 plots the transmitted power as a function of rectangular pinhole acceptance. The total power transmitted by a 30 μrad by 30 μrad pinhole is 925 W whereas the 20 μrad by 20 μrad pinhole transmits only 420 W. As discussed in Section 4.2.3, 925 W exceeds the power rating of LN-cooled silicon monochromators.

Table 4.2.1: U23 undulator emission envelope as a function of photon energy. The photon beam effective rms opening angle $\sigma_{x'\_eff}$ ($\sigma_{y'\_eff}$) is the quadrature sum of the electron beam $\sigma_{x'}$ ($\sigma_{y'}$) listed in Table 3.1.1 and the diffraction limited photon opening angle $\sqrt{(\lambda/L)}$ where L=3.5m.

E (keV)	$\sigma_{x'\_eff}$ (μrad)	$\sigma_{y'\_eff}$ (μrad)	$3\sigma_{x'\_eff}$ x $3\sigma_{y'\_eff}$
5.0	9.3	8.5	27.9 x 25.5
10.0	7.2	6.0	21.6 x 18.0
20.0	5.8	4.3	17.4 x 12.9
40.0	5.0	3.1	15.0 x 9.3
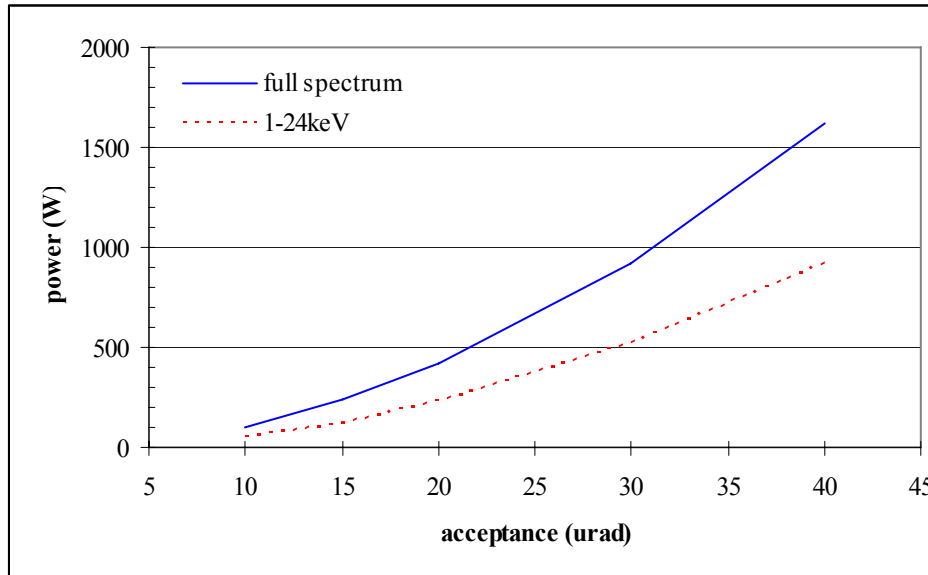
Figure 4.2.2: U23 power at k_{max} transmitted through a rectangular pinhole acceptance for 4.5GeV/1.5A. The solid blue line is integrated over the entire emission spectrum whereas the dashed red line is integrated up to 24 keV as an approximation to the power obtained downstream of a low pass filter mirror.

4.2.2 Mirrors

Introducing a flat mirror in the beam line provides needed power filtering. For example, a Rh-coated mirror operating at 2.7-mrad incident angle cuts off the transmitted spectra for energies greater than the 23.2 keV Rh k-edge. Integrating the beam transmitted through a 30-μrad pinhole up to 24 keV shows that such a mirror reduces the downstream power to 520 W. The remaining 405 W is deposited in the mirror at an average power density of approximately 0.3 W/mm^2 which does not present a significant thermal deformation concern. Finite element analyses of water-cooled silicon mirrors with cross-sections designed to minimize thermal distortion indicate

the thermal figure distortion is less than 0.7 μrad rms for a more demanding 0.5 W/mm^2 and 600-W absorbed power load. (<0.1μrad rms for 0.12W/mm^2 and 140W). Though a more expensive approach, cryogenically-cooled silicon mirrors would eliminate thermal distortion as a source of emittance degradation. While the thermal deformation is not cause for excessive concern, introduction of a mirror can degrade the beam characteristics as addressed in more detail below. Long wavelength figure error can be corrected actively using adaptive mirror technology, but shorter wavelength errors will contribute to emittance and coherence degradation. Since the source horizontal emittance is much larger than the vertical emittance, the beam degradation is less problematic for a horizontally deflecting mirror than a vertically deflecting mirror. A horizontally deflecting mirror is also less subject to gravitational induced figure deformation. The long optical lever arm associated with a mirror located at approximately 65 m (i.e., inside the storage ring concrete shielding) imposes mirror stability requirements that will necessitate active mirror pointing feedback as is practiced at most third generation synchrotron sources.

The 520W transmitted by a 30-μrad pinhole coupled with a 24-keV low pass mirror still exceeds the power that can be managed with existing cryogenically-cooled monochromators without introducing observable crystal thermal distortion. More aggressive aperturing. transmitting only a $3\sigma_{x'eff}$ x $3\sigma_{y'eff}$ beam, helps at higher photon energies but at low energies more effective power filtering is required. For a beam line designed for only low energy applications, a fixed, low-energy cutoff mirror can be used. More generally, a variable cutoff energy mirror system can be devised using two anti-parallel mirrors with variable angle of incidence. By employing an anti-parallel or periscope-like mirror system geometry, the axis of the downstream optics can be fixed independently of the mirror system cutoff energy. Reducing the acceptance to $3\sigma_{x'eff}$ x $3\sigma_{y'eff}$ and employing a variable cutoff mirror system significantly reduces the power transmitted to the monochromator as illustrated in Figure 4.2.3.
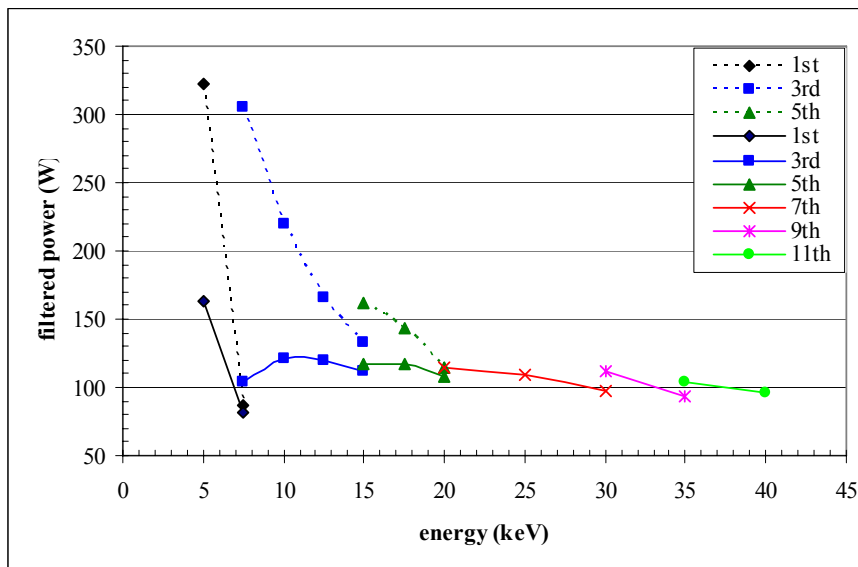
Figure 4.2.3: Transmitted power of U23 along odd harmonic tuning curves with a $3\sigma_{x'eff}$ x $3\sigma_{y'eff}$ aperture and low-pass mirror filtering. The broken lines depict the results for a fixed 24-keV cutoff energy mirror system while the solid lines depict the results for a variable cutoff mirror system adjusted to filter harmonics higher then the specified harmonic.

Introducing a cutoff mirror inside the storage ring offers several side benefits besides power filtering. The suppression of the higher energy portion of the synchrotron spectra and the displacement of the pink synchrotron beam out of the gas Bremsstrahlung cone greatly simplifies beam line shielding. Additionally, the mirror body becomes a source of Compton scatter that can

be monitored to provide vertical beam position information for electron beam steering feedback. This approach, which has been employed successfully on an SSRL undulator beam line, has the virtue of utilizing the core of the undulator beam and minimizing contamination from bend magnet radiation.

4.2.3 Monochromators

Aggressive aperturing and power filtering, as depicted in Figure 4.2.3, limits the power transmitted to the monochromator to 90-125W typical and 165W maximum. Assuming the monochromator is located at 78 m near the downstream end of the FOE, 7-15 W/mm^2 power density is incident on the monochromator first crystal surface for photon energies 5-20 keV with a Si(111) crystal, or 9-16.5 W/mm^2 for 7-40 keV with a Si(220) crystal. The power density variation with tuning and crystal index is shown in Figure 4.2.4. Relocating the monochromator downstream closer to the experimental hutch (~110 m) reduces the power density up to two-fold, but it increases shielding complexity owing to the transport of pink beam from the FOE.
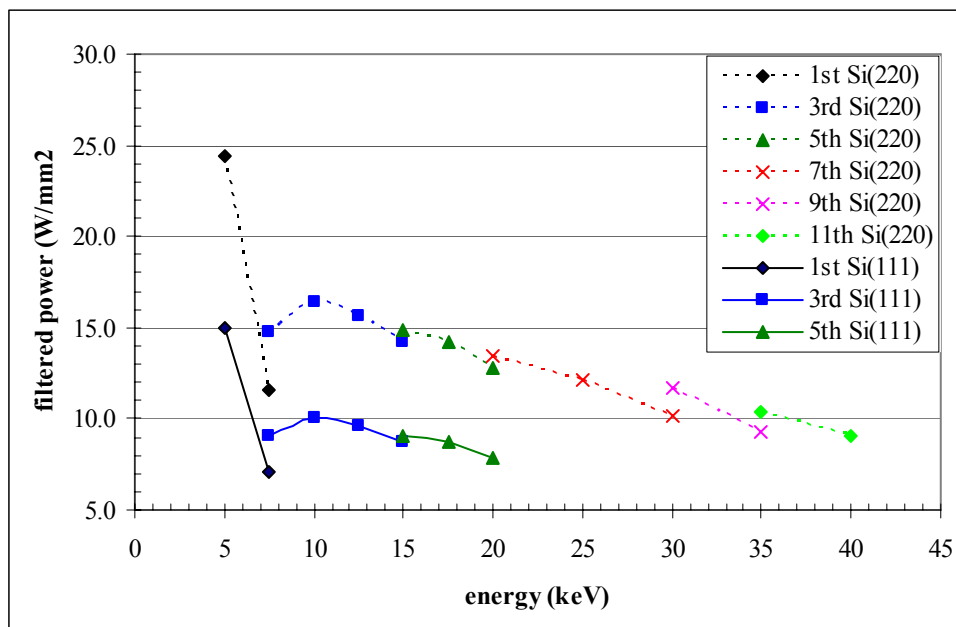
Figure 4.2.4: Power density incident on a U23 monochromator first crystal surface along odd harmonic tuning curves assuming a $3\sigma_{x'eff}$ x $3\sigma_{y'eff}$ aperture and a variable cutoff mirror system adjusted to filter harmonics higher then the specified harmonic. The broken lines represent the power density for a Si(220) crystal while the solid lines depict similar results for a Si(111) crystal.

Cryogenically-cooled monochromator crystals are used extensively on high-power density beam lines at third generation light sources, including SSRL. The internally LN-cooled Si crystals employed in the SSRL LN monochromator have been studied extensively through finite element analysis (FEA) as well as empirically under 500-mA SPEAR3 beam conditions. In particular, the response of these crystals has been calculated for 200-W applied beam power and 8-11 W/mm^2 power footprint geometries similar to that of a PEP-X monochromator. The thermal analyses indicate 95-101 K maximum surface temperatures and 2.3-3.2 μrad rms thermal deformation. The temperature profile of the 11.1 W/mm^2 case is depicted in Figure 4.2.5. The results of the FEA clearly demonstrate that monochromator thermal performance requires improvement in order to preserve the PEP-X emittance. Possible fruitful areas for investigation include improved crystal materials (e.g., isotopically pure diamond) and enhanced cryogenic cooling of silicon whereby the crystal is maintained in a more isothermal state at a temperature closer to that of zero thermal expansion (i.e., ~130 K). It should be noted that SPEAR3 operating at 500 mA

provides a very good platform for monochromator research as "improperly" filtered beams from various SPEAR3 IDs can attain the powers and power densities of Figures 4.2.3 and 4.2.4.
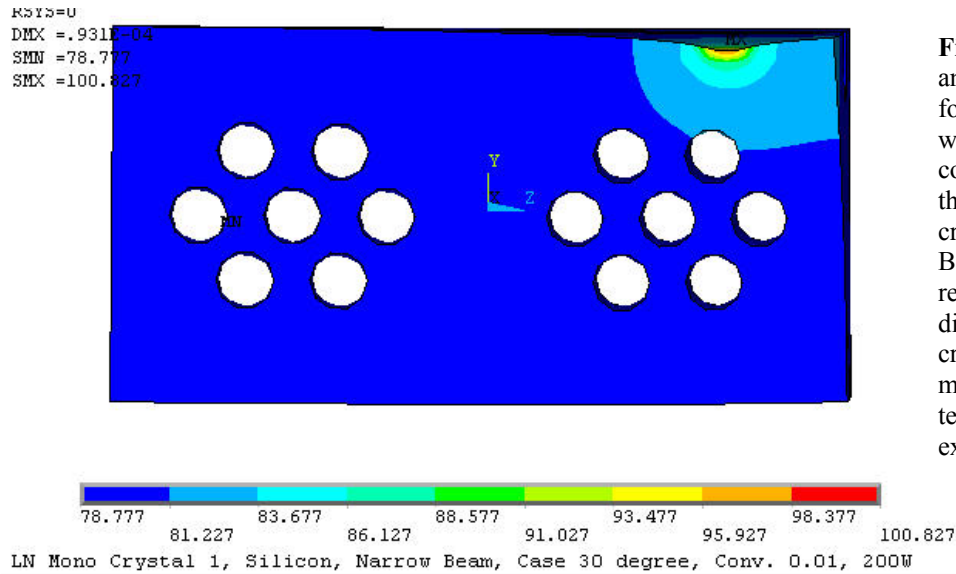
Figure 4.2.5: FEA of 200-W and 11.1-W/mm^2 power footprint on a silicon crystal with liquid nitrogen internal cooling. The calculated thermal distortion of the crystal is 3.17 µrad rms. Both empirical and FEA results indicate that the distortion is reduced if the crystal temperature is maintained closer to the temperature of zero thermal expansion (~130 K).

4.2.4 Downstream Optical Components

Beam power is no longer an engineering issue downstream of the monochromator. Depending on the application, Kirkpatrick-Baez (KB) mirrors, compound refractive lenses, or zone plates may find focusing application. Micro-focusing optical elements of various types are the subject of intense development work as manifest by the rapidly evolving state of the art.

Rather than try to capture the current state of these developments here, we examine a modest demagnification KB mirror system as a simple means to characterize the PEP-X emittance degradation owing to the upstream optics. We assume the use of a 7:1 horizontal demagnification, *perfect* elliptically figured focusing mirror which focuses at 100 m. This places the mirror 12.5 m upstream of the focus. The horizontal emittance degradation of such an optical system is dominated by the power-filtering mirror system located upstream of the monochromator. Reasonably state-of-the-art mirrors can attain slope errors in the 0.25-µrad rms range (i.e., the hard x-ray offset mirror system used for the LCLS). Assuming an anti-parallel, variable cutoff power-filtering mirror system with two flat mirrors, the effective figure error for the composite system will be √2 larger or 0.35 µrad rms. The point-spread function for this system is ~9 µm rms. In contrast, the ideal demagnified source image is 5.2 µm rms. Consequently, the net horizontal emittance degradation is approximately 1.7-fold. This does not describe the entire beam degradation situation since wavefront-distortion effects are not considered. Applying the Maréchal Criterion for wavefront distortion limits the acceptable distortion to λ/14, which, for a two-mirror system, constrains the mirror surface long-wavelength height variation to λ/(28α√2) rms where α is the beam's incident angle on the mirror surface. Assuming 10-keV radiation and 2.7-mrad incident angle yields a mirror surface height control of 12 Å rms. This limitation is about two times more aggressive than mirror vendors currently find

acceptable. A looser 20-Å rms height error specification results in 50% beam intensity reduction of the coherent beam fraction.

Vertical emittance degradation associated with the upstream (i.e., non-focusing) optics is dominated by the monochromator thermal distortion as discussed above. The degradation is energy-dependent owing both to the energy dependence of the monochromator distortion and the energy dependence of the effective source emittance when the diffraction-limited photon phase space is added in quadrature with the electron source phase space. Quantitative prediction of the vertical emittance degradation awaits a more complete study of the monochromator's thermal response to PEP-X power conditions. It is clear, however, that improved monochromator thermal performance is essential to realizing the full potential of PEP-X.

4.2.5 Beam Line Design Challenges

Given the afore mentioned emittance and phase distortion effects with current beam line technology, it is appropriate to list areas where technological improvements could deliver important beam line cost and/or performance advantages:

- Improved thermal designs could reduce masking costs and provide more beam line layout flexibility.

- Improved mirror cooling technologies couls reduce emittance degradation and improve beam stability.

- Improved mirror polish/figures would reduce emittance and coherence degradation.

- Advanced beam position and shape monitors would enhance beam stability when incorporated into feedback systems.

- Reduced thermal deformation of monochromator crystals through cooling improvements and/or alternative crystals would reduce emittance and coherence degradation as well as improve beam stability. Substantial improvements in power management could eliminate the need for power filtering mirrors. Though not explicitly discussed above, grating monochromators for VUV and soft x-ray beam lines would derive similar benefits from improved thermal performance.

- Advances in micro-focusing optics, such as smaller zone plate line widths, would enhance mircroscope resolution.

- Improvements in optics support and experimental hall floor stability would reduce beam instability.

- Enhancements in permanent magnet and/or superconducting magnet technology could increase source brightness.

Acknowledgments

References

[1]   H. Wiedemann, "PEP as a Dedicated Synchrotron Light Source", SSRL ACD Note 16, July 1984.

[2]   H. Winick, R. Coisson, Proceedings of the Workshop on PEP as a Synchrotron Radiation Source, Oct 20-21, 1987, SSRL/SLAC.

[3]   H. Wiedemann, "An Ultra-Low Emittance for PEP Using Damping Wigglers", NIM A266, 1988.

[4]   L. Emery, PhD thesis, 1991.

[5]   A. Ropert, J.M. Filhol, P. Elleaume, L. Farvacque, L. Hardy, J. Jacob, U. Weinrich, "Towards the Ultimate Storage Ring-Based Light Source", Proc. EPAC 2000, Vienna.

[6]   G. Hoffstaetter, "Toward an Energy Recovery Linac X-ray Source at Cornell University", presented at the ICFA FLS 2006 Workshop, http://epaper.kek.jp/fls06/TALKS/WG203_TALK.PDF , Hamburg, 2007.

[7]   H.-D. Nuhn, R. Tatchyn, H. Winick, A. Fisher, J. Gallardo, C. Pellegrini, "Short Wavelength FELs on Large Storage Rings", NIM in Phys. Res. A, 1992.

[8]   J. Wang and S. Tantawi, "X-Band Traveling Wave Structure for Ultra-Fast RF Kicker", SLAC iinternal note, Aug. 2007.

[9]   V. Dolgashev, "Crab Cavities", SLAC internal note, Aug. 2007.

[10] K. Bane, Y. Cai, A. Chao, R. Hettel, Z. Huang, Y. Nosochkov, G. Stupakov, L. Wang, M.-H. Wang, "Lattice and Collective Effects for PEP-X", SLAC-PUB-13225, April 2008.

[11] K. Bane, Y. Nosochkov, SLAC internal note on lattice parameters, IBS and Touschek lifetime at 3.5, 4.0 and 4.5 GeV, June 2008.

[12] Z. Huang, "SASE and Seeded FELs using Stored PEP Beams", SLAC internal note, April 17, 2008.

[13] C. Pellegrini, "Injected Beam First-Turn Lasing on PEP", SLAC internal note, April 2008.

[14] X. Huang, "Ultra-Short Bunches in Future PEP" and appendix "Slice Emittance Evolution Ultra-Short Bunches", SLAC internal reports, August 2007.

[15] S. Tantawi, "RF Undulators for Storage Rings", SLAC internal report, April 2008.

[16] M. Tischer, K. Balewski, M. Seidel, L. Yongjun, P. Vobly, V. Kuzminykh, A. Krasnov, K. Zolotariov, E. Levichev, "Status of the PETRA III Damping Wigglers", Proc. 2006 EPAC, Edinburgh, p. 3565.

[17] H. Schwarz, R. Rimmer, "RF System Design for the PEP-II B Factory", Proc. 1994 EPAC, London p. 1882.

[18] P. Marchand, "Possible Upgrading of the SLS RF System for Improving Beam Lifetime", Proc. 1999 Part. Accel. Conf., New York, NY, p. 989.

[19] P. vom Stein, M. Pekeler, H. Vogel, W. Anders, S. Belomestnykh, J. Knobloch, H. Padamsee, "A Superconducting Landau Accelerator Module for BESSY II", Proc. 2001 Part. Accel. Conf., Chicago, Ill, p. 1175.

[20] J.M. Byrd and M. Georgsson, "Lifetime increase using passive harmonic cavities in synchrotron light sources", PRST-AB 4, 030701 (2001).

[21] K. Wittenburg, "The Beam Diagnostic Instrumentation of PETRA III", Proc. of the 2008 Beam Instrumentation Workshop, Lake Tahoe, May 2008.

[22] D. Shu, E.E. Alp, J. Barraza, T.M. Kuzay, T. Mooney, "Optical Design for Laser Doppler Angular Encoder with Subnanoradian Sensitivity", www.aps.anl.gov/Science/Reports/1999/alpe4.pdf

[23] Z. Huang, "Y-Z Emittance Exchange in PEP3", SLAC internal report, November 2006.